Transition metal complexes with chirality at the metal as well as chiral ligands

M.Sc. Research Thesis

By

Subhabrato Chowdhury



DEPARTMENT OF CHEMISTRY INDIAN INSTITUTE OF TECHNOLOGY INDORE MAY 2025

Transition metal complexes with chirality at the metal as well as chiral ligands

A THESIS

Submitted in partial fulfilment of the requirement for the award of the degree

of

Master of Science

by

Subhabrato Chowdhury

Roll no. 2303131028



DEPARTMENT OF CHEMISTRY INDIAN INSTITUTE OF TECHNOLOGY INDORE MAY 2025



INDIAN INSTITUTE OF TECHNOLOGY INDORE

CANDIDATE'S DECLARATION

I hereby certify that the work which is being presented in the thesis entitled "Transition metal complexes with chirality at the metal as well as chiral ligands," in the partial fulfilment of the requirements for the award of the degree of MASTER of SCIENCE and submitted to the DEPARTMENT of CHEMISTRY, Indian Institute of Technology Indore, is an authentic record of my work carried out during the period July 2024 to May 2025 under the supervision of Dr. Amrendra K. Singh, Department of Chemistry, Indian Institute of Technology Indore. The matter presented in this thesis has not been submitted by me for the award of any other degree of this or any other institute.

Subhabrato Chowdhury

Signature of the Student

This is to certify that the above statement made by the candidate is correct to the best of my/our knowledge.

Dr. Amrendra K. Singh

Signature of the M.Sc. Thesis Supervisor

Subhabrato Chowdhury has successfully given his M. Sc. oral Examination held on 14/05/2025.

Signature of supervisor of M. Sc Thesis

Date: 20/5/2025

ACKNOWLEDGEMENTS

Initially, I would like to express my heartfelt gratitude to my thesis supervisor, **Dr. Amrendra Kumar Singh**, for his invaluable guidance, insightful suggestions, and dedicated supervision. His constant encouragement has been instrumental throughout my research journey. I am also deeply thankful to the members of my **PSPC** committee members, **Dr. Abhinav Raghuvanshi** and **Prof. Shaikh M. Mobin** for their significant contributions and support.

My sincere appreciation extends to the **Department of Chemistry** at IIT Indore for providing me with the opportunity and resources to pursue this research. I am especially grateful to **Prof. Tushar Kanti Mukherjee**, Head of the Department of Chemistry, for his unwavering support and encouragement.

I would also like to acknowledge the faculty members and the staff of the Sophisticated Instrumentation Center at IIT Indore, whose cooperation and assistance have been vital to the successful completion of this dissertation.

Also, I would like to extend my thanks to my seniors, **Ms. Achena saha** (Ph.D. scholar) and **Ms. Ekta Yadav** (Ph.D. scholar), for their unwavering support, insightful guidance, and encouragement, all of which have significantly enhanced both this project and my overall academic journey. I am profoundly grateful to my brothers for their unwavering support and belief in me through every stage of my life. Lastly, I owe my deepest appreciation to my parents, whose encouragement and support have been the foundation of all my achievements.

Subhabrato Chowdhury M. Sc. 2nd year Roll No. 2303131028 Department of Chemistry

Dedicated to my Parents

ABSTRACT

Chiral ruthenium N-heterocyclic carbene (NHC) complexes form a diverse and versatile class of organometallic compounds with a wide range of structural variations and applications. This study presents our attempts on the separation of diastereomers of thermally stable octahedral Ru(II)-CNC pincer complexes. However, diastereomer separation proved unsuccessful utilizing camphor sulfonate as a chiral auxiliary. Consequently, the approach shifted towards pre-reported Ru(II)-NHC-DMSO and Ru(II)-NHC-DMS complexes² alternative chiral auxiliaries, including R-BINAP, S-BINAP, S-BINAM, and R-BINAM. Both photochemical and thermal synthetic routes were explored. ¹H NMR spectroscopy indicated a 3:1 diastereomeric ratio, though repeated attempts at physical separation were unsuccessful, so far. All complexes were thoroughly characterized using ¹H, ¹³C, and ³¹P NMR spectroscopy. The broad utility of chiral Ru-NHC complexes stems from their customizable steric and electronic environments, which make them highly suitable for fine-tuning in asymmetric catalysis and bioinorganic chemistry. Ongoing research is directed at expanding their applications and deepening the understanding of structure-property relationships.

TABLE OF CONTENTS

LIST OF FIGURES	XI-XII
LIST OF SCHEMES	XIII
ACRONYMS	XIV
NOMENCLATURE	XV
CHAPTER 1: INTRODUCTION	1-8
1.1 Aim of the experiment	1
1.2 General Introduction	1-2
1.3 N-Heterocyclic carbene	3-5
1.4 Chiral Ruthenium N-Heterocyclic carbene(NHC) complexes	6-7
1.5 Chiral Auxiliary	7-8
CHAPTER 2: EXPERIMENTAL SECTION	8-21
2.1 General information	8-9
2.2 Chemicals and reagents	9
2.3. Instrumentation	9
2.4.1 Synthesis of Ligand L1	9-10
2.4.2 Synthesis of Ligand L1.HI	10
2.4.3 Synthesis of Ligand L2	10
2.4.4 Synthesis of Ligand L3	11
2.4.5 Synthesis of Ligand L4	11
2.5.1 Synthesis of Precursor P1	11-12
2.5.2 Synthesis of Precursor P2	12
2.5.3 Syntesis of Precursor P3	12-13
2.5.4 Synthesis of Precursor P4	13
2.5.6 Synthesis of Precursor P5	13-14
2.5.7 Synthesis of Complex Ru1 and Ru1'	14-16
2.5.8 Synthesis of Complex Ru2 and Ru2'	16
2.5.9 Synthesis of Complex Ru3 and Ru3'	17-18
2.6.0 Synthesis of Complex Ru4 and Ru4'	18
2.6.1 Synthesis of Complex Ru5 and Ru5'	18
2.6.2 Synthesis of Complex Ru6 and Ru6'	19
2.6.3 Synthesis of Complex Ru7 and Ru7'	19-20

2.6.4 Synthesis of Complex Ru8 and Ru8'	20-21
CHAPTER 3: RESULTS AND DISCUSSION	21-51
3.1 Characterization of Ligands	32-37
3.2 Characterization of Precursors	37-42
3.3.1 Characterization of Complex Ru1 and Ru1'	43-44
3.3.2 Characterization of Complex Ru2 and Ru2'	45
3.3.3 Characterization of Complex Ru3 and Ru3'	46
3.3.4 Characterization of Complex Ru4 and Ru4'	46-47
3.3.5 Characterization of Complex Ru5 and Ru5'	47-48
3.3.6 Characterization of Complex Ru6 and Ru6'	48
3.3.7 Characterization of Complex Ru7 and Ru7'	49
3.3.8 Characterization of Complex Ru8 and Ru8'	50-51
CHAPTER 4: CONCLUSION AND FUTURE PERSPECTIVE	52-53
4.1 Conclusion	52
4.2 Future Perspective	53
REFERENCES	54-59

LIST OF FIGURES

- Fig.1: N-Heterocyclic carbenes
- Fig.2: Stabilization of the carbene by adjacent

ring nitrogens

- Fig.3: First stable N-Heterocyclic carbene
- **Fig.4:** The structures of the chiral Ruthenium(II)

Complexes

- Fig.5: Chiral auxiliary binding process
- Fig.6: Overall strategy for the Chiral-Auxiliary

Mediated asymmetric synthesis of Ruthenium

NHC complexes

- Fig.7: LCMS of Ligand L1.HI
- Fig.8: ¹H NMR of Ligand L1.HI
- Fig.9: ¹³C NMR of Ligand L1.HI
- Fig.10: LCMS of Ligand L2
- Fig.11: LCMS of Ligand L3
- Fig.12: ¹H NMR of Ligand L3
- **Fig.13:** ¹³C{¹H} NMR of Ligand L3
- Fig.14: LCMS of Ligand L4
- Fig.15: ¹H NMR of Ligand L4
- **Fig.16:** ¹³C{¹H} NMR of Ligand L4
- Fig.17: LCMS of Precursor P1
- Fig.18: UV-Vis spectra of Precursor P1
- Fig.19: LCMS of Precursor P2
- Fig.20: UV-Vis spectra of Precursor P2
- Fig.21: ¹H NMR of Precursor P3
- Fig.22: ¹³C{¹H} NMR of Precursor P3
- Fig.23: ³¹P{¹H} NMR of Precursor P3
- Fig.24: LCMS of Precursor P4
- Fig.25: ¹H NMR of Precursor P4
- Fig.26: LCMS of Precursor P5
- Fig.27: LCMS of Complex Ru1 and Ru1'

Fig.28: LCMS of Complex Ru3 and Ru3'

Fig.29: ¹H NMR of Complex Ru4 and Ru4'

Fig.30: ¹³C{¹H} NMR of Complex Ru4 and Ru4'

Fig.31: ¹H NMR of Complex Ru5 and Ru5'

Fig.32:¹³C{¹H} NMR of Complex Ru5 and Ru5'

Fig.33: ¹H NMR of Complex Ru6 and Ru6'

Fig.34: $^{13}C\{^{1}H\}$ NMR of Complex Ru6 and Ru6'

Fig.35: ¹H NMR of Complex Ru7 and Ru7'

Fig.36: ¹³C{¹H} NMR of Complex Ru7 and Ru7'

Fig.37: ¹H NMR of Complex Ru8 and Ru8'

Fig.38: ¹³C{¹H} NMR of Complex Ru8 and Ru8'

Fig.39: ³¹P{¹H} NMR of Complex Ru8 and Ru8'

List of Schemes

Scheme 1. Synthesis of ligand L1

Scheme 2. Synthesis of ligand L1.HI

Scheme 3. Synthesis of ligand L3 and L4

Scheme 4. Synthesis of Precursor P1 and P2

Scheme 5. Synthesis of Precursor P3

Scheme 6. Synthesis of Precursor P4

Scheme 7. Synthesis of Precursor P5

Scheme 8. Synthesis of complex Ru1 and Ru1'

Scheme 9. Synthesis of complex Ru2 and Ru2'

Scheme 10. Synthesis of complex Ru3 and Ru3'

Scheme 11. Synthesis of complex Ru4 and Ru4'

Scheme 12. Synthesis of complex Ru5 and Ru5'

Scheme 13. Synthesis of complex Ru6 and Ru6'

Scheme 14. Synthesis of complex Ru7 and Ru7'

Scheme 15. Synthesis of complex Ru8 and Ru8'

ACRONYMS

ACN Acetonitrile

CAN Ceric ammonium nitrate

CDCl₃ Chloroform-d

CHCl₃ Chloroform

DCM Dichloromethane

DMSO Dimethyl sulfoxide

ESI Electron spray ionization

HRMS High-resolution mass spectrometry

K₂CO₃ Potassium carbonate

LCMS Liquid chromatography-mass spectrometry

MeOH Methanol

Na₂SO₄ Sodium sulfate

NMR Nuclear magnetic resonance

NH₄Cl Ammonium chloride

TLC Thin layer chromatography

BINAM 1,1'-Binaphthyl-2,2'-diamine

BINAP 2,2'-Bis(diphenylphosphino)-1,1'-binaphthalene

NOMENCLATURE

°C Degree Celsius

h hour Hz Hertz M Molar

Millilitre mL

Milligrams mg

megahertz MHz millimole

mmol

Nanometer nm

Parts per million ppm

CHAPTER 1

INTRODUCTION

1.1 Aim of the project:

This research focuses on synthesizing and characterizing diastereomerically pure Ruthenium(II) complexes containing N-heterocyclic carbene (NHC) ligands. We aim to develop synthetic methods utilizing enantiomerically pure chiral auxiliary ligands-specifically (R)- and (S)-BINAP (2,2'-bis(diphenylphosphino)-1,1'-binaphthyl) and (R)- and (S)-BINAM (1,1'-binaphthyl-2,2'-diamine)-to create well-defined stereochemical environments around the ruthenium center. Diastereomeric purity will be evaluated using NMR spectroscopy, X-ray crystallography and circular dichroism. These stereochemically defined Ru(II)-NHC complexes have potential applications in asymmetric catalysis, where precise spatial control is essential for achieving high stereoselectivity in chemical transformations.³

1.2 General Introduction:

Chiral ruthenium complexes are a fascinating class of organometallic compounds that have garnered significant attention due to their unique stereochemical properties and versatile applications in both chemical synthesis and biological systems.⁴ The chirality in these complexes commonly arises from the octahedral coordination geometry of the ruthenium center, which allows for the formation of nonsuperimposable mirror-image isomers known as enantiomers. Specifically, the Δ (delta) and Λ (lambda) diastereomers are the two most prominent stereoisomers found in such complexes.⁵ These designations refer to the helical twist of the ligands around the ruthenium center: the Δ isomer has a right-handed (clockwise) configuration, while the Λ isomer exhibits a left-handed (counterclockwise) twist.⁶⁻⁷ The spatial arrangement of these ligands imparts distinct chiral environments to the complexes, which can profoundly influence their chemical reactivity and interactions with other chiral molecules.8

One of the most studied examples is the family of tris-chelated ruthenium(II) complexes, such as $[Ru(phen)_3]^{2+}$ (where phen = 1,10-phenanthroline). The Δ and Λ forms of these complexes have been shown to interact differently with biological macromolecules like DNA.⁹ For instance, the Δ isomer often displays selective binding to the minor groove of DNA, particularly favouring AT-rich regions, while the Λ isomer may interact more broadly or with different sequence specificity. This stereoselective recognition is crucial for the development of ruthenium-based probes and drugs that target nucleic acids.

Beyond biological recognition, chiral ruthenium complexes have become indispensable tools in asymmetric catalysis. ¹⁰ The introduction of chiral ligands-such as tetradentate PNNP (phosphine-nitrogen-nitrogen-phosphine) or helical bapbpy (bis(aminopyridine)-bipyridine) frameworks-enables precise control over the spatial arrangement of reactants during catalytic transformations. ¹¹ This control is essential for achieving high levels of enantioselectivity in reactions like asymmetric hydrogenation, cyclopropanation, and C–H amination. In these processes, the chiral-at-ruthenium center can stabilize specific transition states, leading to the preferential formation of one enantiomer over the other in the product. Furthermore, recent advances have shown that modifying the steric and electronic properties of the ligands can tune the inversion barriers of the helical chirality, allowing for the isolation of configurationally stable ruthenium complexes. ¹²

The versatility of chiral ruthenium complexes extends to their ability to mediate challenging transformations, such as nitrene insertion and enantioselective macrocyclization, which are valuable in the synthesis of complex molecules and pharmaceuticals.¹³ Their robust structural frameworks and tuneable chiral environments make them attractive candidates for designing new catalysts and functional materials. Overall, the unique stereochemistry and broad applicability of chiral ruthenium complexes continue to drive innovation in both synthetic chemistry and the development of novel biomolecular tools.

1.3 N-Heterocyclic carbene (NHC):

N-Heterocyclic carbenes (NHCs) are a class of organic compounds characterized by the presence of a divalent carbon atom (carbene center) embedded within a heterocyclic ring system.¹⁴ What makes NHCs especially interesting is that the carbene carbon is bonded to two nitrogen atoms commonly arranged in five or six-membered rings creating a stable heterocyclic framework. These nitrogen atoms play a critical role in delocalizing electron density and stabilizing the carbene center through resonance and inductive effects. The most common NHC framework is based on the imidazolium ring, forming what is known as imidazolylidenes. Other well-known structures include triazolylidenes, which are derived from triazole rings, and benzimidazolylidenes, which incorporate a benzene-fused imidazole. These heterocyclic systems not only stabilize the carbene center but also influence the electronic and steric properties of the molecule, which can be fine-tuned through substituents on the nitrogen atoms and the ring backbone.

NHCs are known for being strong σ-donor ligands, often outperforming traditional phosphine ligands (PR₃) in this respect.¹⁵ Their ability to donate electron density to metal centers makes them ideal ligands in organometallic chemistry, where they help stabilize metal complexes, including those with low oxidation states or high reactivity.¹⁶ This exceptional electron-donating ability enhances the catalytic efficiency and stability of the metal complexes they form. In contrast to traditional carbenes, which are typically transient and highly reactive, NHCs are thermodynamically stable.¹⁷ This stability was once thought unattainable until the landmark work of Anthony Arduengo and Guy Bertrand in the late 20th century. They successfully isolated the first stable NHCs, challenging long-standing assumptions in organic

chemistry and opening new frontiers in both theoretical and applied research.

Carbenes, defined as neutral species with a bivalent carbon atom possessing a sextet of electrons (i.e., lacking a full octet), have fascinated chemists since the late 19th century. Early indirect evidence of their existence came from the pioneering studies of Buchner and Curtius, and later Staudinger and Kupfer, who laid the foundation for modern carbene chemistry. However, it wasn't until the development of stable carbenes in the 1980s and 1990s that the field experienced a renaissance. Arduengo's synthesis of the first stable crystalline NHC marked a turning point, transforming carbenes from fleeting intermediates into isolable, functional species. The emergence of Nheterocyclic carbenes (NHCs) has significantly transformed the landscape of homogeneous catalysis, making them indispensable ligands in numerous transition-metal-catalyzed reactions. 18 Their strong σ-donating ability allows NHC metal complexes to efficiently promote a range of transformations, including cross-coupling reactions such as Suzuki-Miyaura, Heck, and Stille couplings, which are widely used for constructing carbon-carbon bonds. NHCs also play a crucial role in hydrogenation reactions of alkenes and imines, often enabling these processes to proceed under mild conditions. 19 Additionally, they are vital in olefin metathesis reactions, where they stabilize rutheniumbased catalysts like Grubbs catalysts, facilitating the rearrangement of carbon-carbon double bonds.²⁰ Beyond their coordination to metals, NHCs have also gained prominence in organocatalysis as nucleophilic carbenes. In this metal-free context, they activate carbonyl compounds such as aldehydes and esters through the formation of reactive intermediates like the Breslow intermediate. ²¹ These intermediates are pivotal in enabling key transformations such as Stetter reactions, benzoin condensations, and umpolung reactions, the latter of which reverses the typical electrophilic nature of carbonyl carbons. This rapidly growing area of organocatalytic carbene catalysis has provided powerful new tools for synthetic chemists, enabling the efficient construction of structurally complex, stereochemically defined, and

functionally diverse organic molecules under environmentally benign conditions. Here some examples of N-Heterocyclic carbenes:

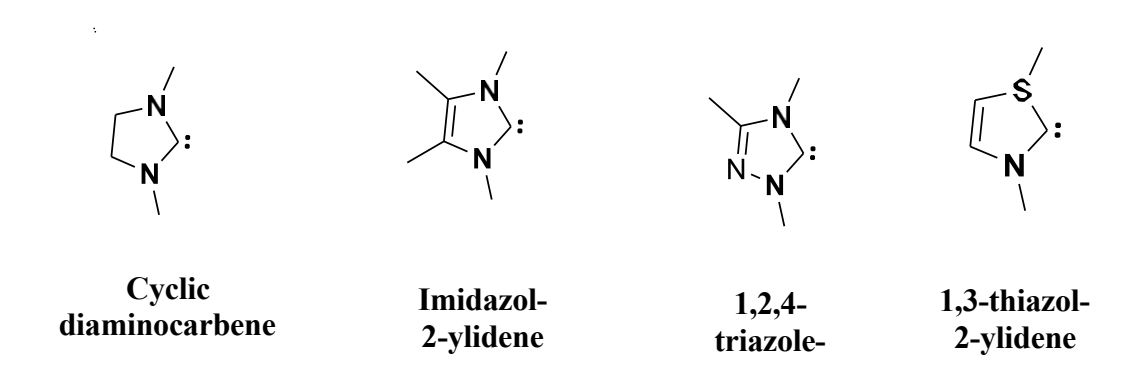


Fig.1: N-Heterocyclic carbenes²²

1. N-heterocyclic carbenes (NHCs) are distinguished from highly electron-rich phosphines by their unique σ -donating capabilities and π -accepting characteristics.

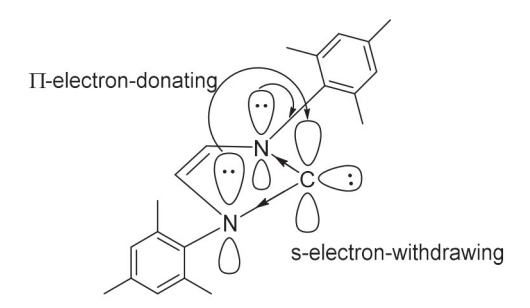


Fig 2. Stabilization of the carbene by adjacent ring nitrogens ²³

- The structure of NHC ligands can be readily modified to precisely
 adjust their steric bulk and electronic properties, enabling control
 over the reactivity and selectivity in metal-mediated
 transformations.
- Metal-NHC complexes exhibit exceptional thermal stability while offering tunable electronic properties, rendering them particularly valuable candidates for the development of advanced organometallic materials.

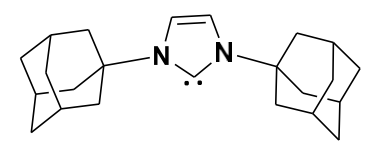


Fig.3: First stable N-Heterocyclic carbene²⁴

1.4 Chiral Ruthenium N-heterocyclic carbene (NHC) complexes:

Chiral Ruthenium N-heterocyclic carbene (NHC) complexes represent a versatile class of organometallic compounds with diverse structural features and applications.²⁵ These complexes can be synthesized through various approaches, including trans metalation from silver precursors and modular assembly from chiral NHCs and diamines.²⁶ They exhibit remarkable structural diversity, featuring both C₁ and C₂ symmetric NHC ligands with various substituents such as N-(S)-phenylethyl groups. Some complexes derive their chirality from the helical arrangement of bidentate ligands around the ruthenium center, creating a stereogenic metal center.²⁷⁻²⁸ Ru-NHC complexes demonstrate exceptional catalytic activity in numerous transformations, including asymmetric hydrogenation of ketones with excellent enantioselectivity, various metathesis reactions (ringclosing, cross-metathesis, and ring-opening polymerization), and nitrene-mediated C-H insertion reactions. Beyond their synthetic applications, these complexes show promising biological activities, exhibiting antimicrobial effects against Gram-positive bacteria and antiproliferative activity against cancer cell lines, sometimes exceeding the potency of standard drugs like cisplatin.²⁹ The versatility of chiral Ru-NHC complexes stems from their tunable steric and electronic properties, which allow for optimization toward specific catalytic or biological applications.³⁰ Chiral Ru-NHC complexes are at the forefront of asymmetric catalysis and bioinorganic chemistry, with ongoing research focused on expanding their applications and understanding how their structure controls their remarkable properties.³¹

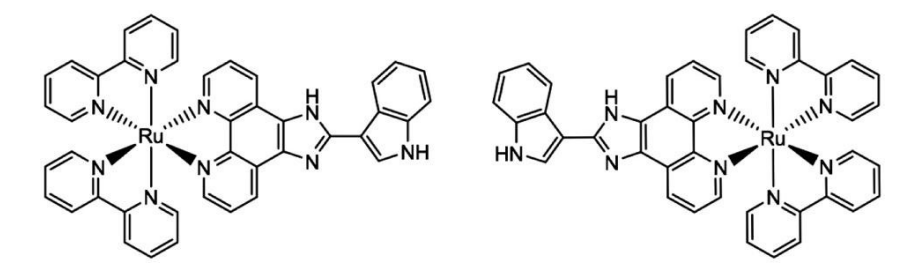


Fig.4: The structures of the chiral ruthenium(II) complexes³²

1.5 Chiral Auxiliary:

A chiral auxiliary is a stereogenic unit temporarily attached to a substrate to control the stereochemical outcome of a chemical reaction, enabling the selective synthesis of one enantiomer over another. This strategy is widely used in asymmetric synthesis, especially when catalytic enantioselective methods are unavailable or less effective. 33-35 The chiral auxiliary is covalently bonded to the substrate, inducing diastereoselectivity in subsequent reactions. After the desired transformation, the auxiliary is removed under mild conditions, ideally without racemization, and can often be recovered and reused. The process generally involves three steps:

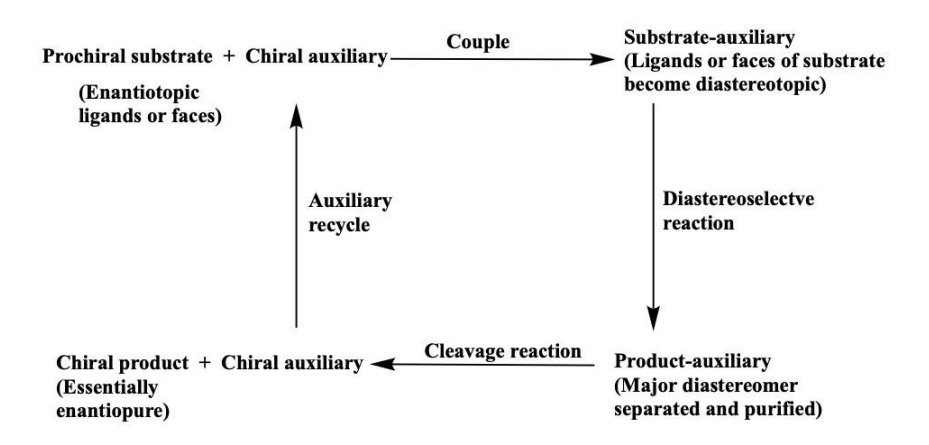


Fig.5: Chiral auxiliary binding process ³⁶

Chiral auxiliaries are essential in the synthesis of pharmaceuticals and complex natural products, as they enable the production of single-enantiomer compounds that are often necessary for biological activity. They offer reliable and predictable control over stereochemistry, making

them especially useful when catalytic asymmetric methods are not available.³⁷ However, their use requires stoichiometric amounts-meaning they are not catalytic-and involves extra steps for both attachment and removal from the target molecule.³⁸⁻⁴⁰ Despite these limitations, chiral auxiliaries remain a foundational tool in asymmetric synthesis, valued for their robustness and effectiveness in constructing complex molecules with defined stereochemistry. Their versatility and proven success ensure they continue to play a significant role in synthetic organic chemistry, even as new catalytic asymmetric methods are developed.⁴¹⁻⁴⁵

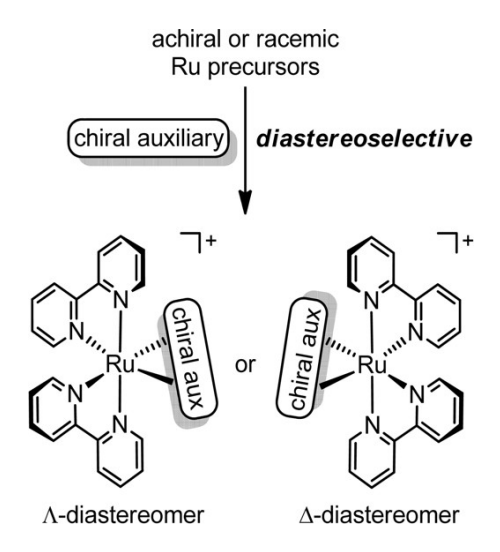


Fig.6: Overall Strategy for the Chiral-Auxiliary-Mediated Asymmetric Synthesis of Ruthenium NHC Complexes ⁴⁶

CHAPTER-2

EXPERIMENTAL SECTION

2.1 General information:

All chemicals and solvents utilized in this study were obtained from commercially available sources and used without further purification, except for hexane and ethyl acetate, which were distilled prior to use. All experiments were carried out under a nitrogen atmosphere using a Schlenk line. Reaction progress was monitored by thin-layer chromatography (TLC) on Merck 60 F254 precoated silica gel plates.

Product purification was achieved by column chromatography on silica gel (100–200 mesh).

2.2 Chemicals and Reagents:

All reagents and solvents used in this experiment were sourced commercially and employed without further purification. These chemicals include Benzimidazole (SRL, 99%), imidazole (SRL, 99%), 2,6- dibromo pyridine (Alfa Aesar, 98%), 2-bromo pyridine (Spectrochem, 99%), potassium carbonate (SRL, 99.5%), sodium

bicarbonate (SRL, 99.5%), ruthenium trichloride trihydrate (SRL), potassium hydroxide (Emplura, 85%), Sodium hydroxide (Emplura,84%), Methyl iodide (Spectrochem, 99%), Isopropyl bromide (Spectrochem, 99%), 1-Methlyimidazole (Spectrochem, 99%), S-BINAM (BLD pharm 98%), R-BINAM (BLD pharm 98%), S-BINAP(BLD pharm 98%) and R-BINAP (BLD pharm 98%).

2.3 Instrumentation:

NMR spectra were recorded at room temperature using Bruker BioSpin ADVANCE III 400 and 500 MHz Ascend instruments. Mass spectrometric analyses were performed on a Bruker-Daltonics micro TOF-Q II mass spectrometer.

2.4 SYNTHESIS OF LIGANDS:

2.4.1 Synthesis of Ligand L1:

Experimental procedure:

A 100 mL two-neck round-bottom flask equipped with a magnetic stirring bar was charged with CuI (0.04 mol, 7.6 g), 2,6-dibromopyridine (0.01 mol, 2.368 g), K₂CO₃ (0.06 mol, 8.29 g), TEMED (2.43 mL), and imidazole (0.04 mol, 2.7 g). DMSO (20 mL) was then added to the reaction mixture at room temperature under a nitrogen atmosphere, after which the flask was sealed and stirred in a preheated oil bath at 120 °C. After 24 hours, the reaction mixture was allowed to cool to room temperature. The mixture was then filtered

using a filtration flask. Following this, brine solution was added to the filtrate (reaction mixture), and extraction was performed with DCM. The organic layer was collected and evaporated using rotary evaporation to yield a white solid with a 75% yield (2.3 g); LCMS (ESI) *m/z* calculated for [M+H]⁺ 211.0913, found 211.0959.

2.4.2 **Synthesis of Ligand L1.HI:**

Experimental procedure:

2-bromopyridine (1.81 mL, 18.98 mol), A Schlenk tube equipped with a magnetic stirring bar was charged with MeI (0.5 mL) and 2,6-di(1H-imidazol-1-yl)pyridine (2.369 mmol, 0.5 g). Dry toluene (5 mL) was then added to the reaction mixture at room temperature under a nitrogen atmosphere. The oil bath temperature was subsequently set to 110 °C, and the reaction was allowed to proceed for 18 hours. Afterward, the precipitate was filtered and further purified through recrystallization to obtain product L1.HI as a yellow solid with an 86% yield (0.429g); **LCMS (ESI)** m/z calculated for [M+H]⁺ 226.113, found 211.1259. ¹H NMR (500 MHz, DMSO-d6) δ 10.26 (s, 1H), 8.85 (s, 1H), 8.69 (d, 1H), 8.39 (t, J= 8.1 Hz, 1H), 8.21 (s, 1H), 8.02 (d, J= 8.1 Hz, 1H), 7.95 (d, J= 7.9 Hz, 1H), 7.20 (s, 1H), 4.00 (s, 2H); ¹³C NMR (126 MHz, DMSO-d6, 25 °C) δ 147.8, 145.2, 144.1, 136.0, 135.9, 130.7, 125.0, 119.1, 117.0, 114.2, 113.0, 111.0, 36.

2.4.3 **Synthesis of Ligand L2:**

Experimental procedure:

2-bromopyridine (1.5799 g, 0.010 mol) and 1*H*-imidazole (2.042 g, 0.030 mol) were charged in a pressure tube at 190 °C in a silicon oil bath for 18h. After completion, the mixture was extracted with DCM and water. After the rotary evaporator, a clear solution was kept in a vacuum. The obtained product was 95% (1.567 g), and the characterization for **LCMS** (ESI) *m/z* calculated for C₈H₇N₃ [M+H]⁺ 146.0713, found 146.0859.

2.4.4 Synthesis of Ligand L3:

Experimental procedure:

A Pressure tube equipped with a magnetic stirring bar was charged with methyl iodide (0.01 mol, 1 mL), along with **L2** (0.01 mol, 1.5 g). Dry toluene (3 mL) was then added to the mixture at room temperature under a nitrogen atmosphere. The reaction mixture was heated in an oil bath at 110 °C for 24 hours. After completion, the precipitate was filtered to afford yellow solids **L3** (80.8% yield).

¹**H NMR** (CDCl₃, 500MHz, 25 °C): δ (ppm) 10.72 (s, 1H), 8.48 (d, 1H), 8.25 (d, 1H), 8.22 (d, 1H),7.98 (d, 1H), 7.82 (dd, 1H), 7.44 (dd, 1H), 4.26 (s, 3H); ¹³**C NMR** (CDCl₃,126 MHz, 25): δ (ppm) 149.25, 145.78, 140.50, 134.83, 125.31, 124.69, 123.70, 119.01, 114.69.

2.4.5 Synthesis of Ligand L4:

Experimental procedure:

A Schlenk tube equipped with a magnetic stirring bar was charged with isopropyl iodide (0.01 mol, 1 mL), along with **L2** (0.01 mol, 1.5 g). Dry toluene (3 mL) was then added to the mixture at room temperature under a nitrogen atmosphere. The reaction mixture was heated in an oil bath at 110 °C for 24 hours. After completion, the precipitate was filtered to afford yellow solids **L4** (62.76% yield), respectively.

¹H NMR (CDCl₃, 500 MHz): δ (ppm) 10.80 (s, 1H), 8.36 (d, 1H), 8.36 (dd, 1H), 8.21 (d, 1H), 7.85 (d, 1H), 7.76 (d, 1H), 5.04 (m, 1H), 1.57 (d, 6H); ¹³C NMR (CDCl₃, 126 MHz, 25 °C): δ (ppm) 148.71, 145.56, 140.11, 133.12, 124.84, 120.85, 119.04,114.72, 53.97.

2.5 SYNTHESIS OF COMPLEXES:

2.5.1 Synthesis of Precursor P1:

Experimental procedure:

A Schlenk tube equipped with a magnetic stirring bar was charged L3 (0.76 mmol, 219.26 mg), RuCl₃·3H₂O (0.76 mmol, 200 mg), and THF (2 mL) under a nitrogen atmosphere. The reaction mixture was stirred at reflux temperature (66 °C) for 12 hours, forming a brown precipitate in a dark brown solution. The resulting brown solid was filtered, washed multiple times with THF, and dried under vacuum to afford P1 (68.8% yield)

For **P1**: (LCMS): 348.93 [M–C1] $^+$, 366.94 [M–C1+H₂O] $^+$. UV-vis λ_{max} /CH₃CN for the Ru-NHC complexes is 384 nm.

2.5.2 Synthesis of Precursor P2:

Experimental procedure:

A Schlenk tube equipped with a magnetic stirring bar was charged L4 (0.76 mmol, 241 mg), RuCl₃·3H₂O (0.76 mmol, 200 mg), and THF (2 mL) under a nitrogen atmosphere. The reaction mixture was stirred at reflux temperature (66 °C) for 12 hours, forming a brown precipitate in a dark brown solution. The resulting brown solid was filtered, washed multiple times with THF, and dried under vacuum to afford P2 (61.15% yield), respectively. For **P2:** (LCMS): 376.96 [M–Cl]⁺. UV-vis λ_{max} /CH₃CN for the Ru-NHC complexes is 385 nm.

2.5.3 Synthesis of precursor P3:

Experimental procedure:

A Schlenk tube equipped with a magnetic stirring bar was charged with **P1** (0.389 mmol, 150 mg), **L1.HI** (0.389 mmol, 137.31 mg), and NaI (0.389 mmol, 58.3 mg). Ethylene glycol (2 mL) was then added to the reaction mixture. The reaction was carried out at reflux temperature (190°C) for 4 hours under a nitrogen atmosphere. After cooling the reaction mixture to room temperature, an aqueous solution of KPF₆ was added, resulting in the formation of an orange precipitate. The precipitate was filtered and purified via column chromatography using 5% MeOH in DCM, yielding a yellowish-orange solid identified as Ru-

3a **60.06% (200 mg);** LCMS **(ESI)** m/z calculated for $[C_{21}H_{20}IN_8Ru]PF_6757.39$, found $[M-PF_6]^+612.99$.

¹H NMR (500 MHz, DMSO-d6) δ 12.96 (s, 1H), 12.28 (s, 1H), 10.17 (d, 1H), 9.70 (d, J = 8.1 Hz, 1H), 8.50 (t, 6H), 8.27 (t, 1H), 8.10 (m, J = 7.9 Hz, 8H), 3.12 (s, 3H), 2.97 (d, 2H); ³¹P NMR (202 MHz, DMSO-d6) δ 133.70, 137.18, 140.73, 144.24, 147.75, 151.27, 154.78; ¹³C NMR (126 MHz, DMSO-d6, 25 °C) δ 187.83, 186.39, 182.01, 153.59, 152.69, 152.09, 141.74, 138.59, 125.60, 122.00, 121.83, 119.93, 118.32, 117.87, 117.73, 112.27, 107.50, 105.19, 104.96, 35.89, 21.96, 15.12.

2.5.4 Synthesis of precursor P4:

Experimental procedure:

A two-neck round-bottom flask was set up in a silicon oil bath at room temperature, and to it were added **P2** (288.5 mg, 0.75 mmol, 1.0 equiv.) and DMSO (2 mL, 0.75 mmol, 1.0 equiv.). The mixture was allowed to react for three days. Upon completion, the mixture was transferred to a vial, where methanol was added to facilitate dissolution. The Deccan process was employed, and the resulting precipitate was subjected to vacuum drying. The obtained product was 53% (0.091 g) and yellow solid. LCMS (ESI) *m/z* calculated for C₁₁H₁₇ClN₃O₂RuS [M-Cl-DMSO+H₂O]⁺ 391.36 found: 391.97, C₁₃H₂₁N₃O₂RuS₂ [M-2Cl+H]⁺ 416.04 found: 416.00.

2.5.4 **Synthesis of precursor P5:**

Experimental Procedure:

Under an Inert atmosphere, in an oven dried Schlenk tube charged with magnetic stirrer bar, the complex **P1** (0.26 mmol) were dissolved in MeOH (2-3ml) and added excess of dimethyl sulphide (1ml). The reaction mixture was refluxed for 6 hours. After the completion of the reaction a clear solution of the reaction a clear solution of the product was obtained. The solvent was triturated using diethyl ether (20ml)

until the solid product is obtained. The final product is dried under vacuum.

Method-a: A Schlenk tube equipped with a magnetic stirring bar was

P5: Yield = 0.056 g (0.123 mmol, 47.4%). LCMS: 419.99 [M-C1]^+ .

2.5.5 Synthesis of complex Ru1 and Ru1':

Experimental Procedure:

charged with P3 (0.023 mmol, 20 mg) and camphor sulfonate (0.023 mmol, 5.84 mg). Acetone was added to the reaction mixture, and the reaction was evidenced by LC-MS (ESI) analysis, in which the calculated m/z value of 717.1548 for [M-PF₆]⁺ was not detected. Method-b: After method-a proved unsuccessful, an alternative approach was adopted. Again, A Schlenk tube equipped with a magnetic stirring bar was charged with P3 (0.023 mmol, 20 mg), camphor sulfonate (0.023 mmol, 5.84 mg) and KPF₆(0.023 mmol, 4.23 mg). ACN was added to the reaction mixture, and the reaction was maintained for 24 hours at room temperature. Upon completion of the reaction, LCMS data was examined, whereby it was determined that the desired product (separation of diastereomeric pairs) was not obtained, as evidenced by LCMS (ESI) analysis, in which the calculated m/z value of 717.1548 for [M-PF₆]⁺ was not detected.

Method-c: When method-b was found to be ineffective, a different method was employed. Again, A Schlenk tube equipped with a magnetic stirring bar was charged with **P3** (0.023 mmol, 20 mg), camphor sulfonate (0.023 mmol, 5.84 mg) and AgPF₆(0.023 mmol, 5.81 mg). ACN was added to the reaction mixture, and the reaction was maintained for 24 hours at reflux temperature. Upon completion of the reaction, LCMS data was examined, whereby it was determined that the desired product (separation of diastereomeric pairs) was not obtained, as evidenced by LCMS (ESI) analysis, in which the calculated m/z value of 717.1548 for [M-PF₆]⁺ was not detected.

Method-d: Following the unproductive outcome of method-c, an alternative procedure was implemented. Again, A Schlenk tube equipped with a magnetic stirring bar was charged with **P3** (0.023 mmol, 20 mg), camphor sulfonate (0.023 mmol, 5.84 mg) and AgPF₆(0.023

mmol, 5.81 mg). Acetone was added to the reaction mixture, and the reaction was maintained for 4 hours at reflux temperature. Upon completion of the reaction, LCMS data was examined, whereby it was determined that the desired product (separation of diastereomeric pairs) was not obtained, as evidenced by LCMS (ESI) analysis, in which the calculated m/z value of 717.1548 for [M-PF₆]⁺ was not detected.

Method-e: When method-d was shown to be unavailing, a substitute method was applied. Again, A Schlenk tube equipped with a magnetic stirring bar was charged with **P3** (0.023 mmol, 20 mg), camphor sulfonate (0.023 mmol, 5.84 mg) and AgPF₆(0.023 mmol, 5.81 mg). Acetone was added to the reaction mixture, and the reaction was maintained for 24 hours at room temperature. Upon completion of the reaction, LCMS data was examined, whereby it was determined that the desired product (separation of diastereomeric pairs) was not obtained, as evidenced by LCMS (ESI) analysis, in which the calculated m/z value of 717.1548 for [M-PF₆]⁺ was not detected.

Method-f: After method-e did not yield the desired results, another strategy was utilized. Again, A Schlenk tube equipped with a magnetic stirring bar was charged with **P3** (0.023 mmol, 20 mg), camphor sulfonate (0.023 mmol, 5.84 mg) and AgPF₆(0.023 mmol, 5.81 mg). Methanol was added to the reaction mixture, and the reaction was maintained for 24 hours at room temperature. Upon completion of the reaction, LCMS data was examined, whereby it was determined that the desired product (separation of diastereomeric pairs) was not obtained,

as evidenced by LCMS (ESI) analysis, in which the calculated m/z value of 717.1548 for [M-PF₆]⁺ was not detected.

Method-g: Once method-f was determined to be fruitless, a new method was pursued. Again, A Schlenk tube equipped with a magnetic stirring bar was charged with **P3** (0.0116 mmol, 10 mg), silver salt of camphor sulfonate (0.0116 mmol, 3.96 mg) in acetone (2 mL). The reaction was maintained for 24 hours at reflux temperature. Upon completion of the reaction, LCMS data was examined, whereby it was determined that the desired product (separation of diastereomeric pairs) was not obtained, as evidenced by LCMS (ESI) analysis, in which the calculated m/z value of 717.1548 for [M-PF₆]⁺ was not detected. Also this modification similarly produced negative results according to LC-MS analysis. Additionally, an ion exchange approach utilizing an aqueous solution of camphor sulfonate was explored, yet this method

likewise proved unsuccessful in achieving the intended separation, as confirmed by LC-MS (ESI) m/z measurements.

2.5.6 Synthesis of complex Ru2 and Ru2':

Experimental Procedure:

After a negative result was obtained using precursor **P3**, a new precursor, P4, which had already been synthesized in our lab, was used. As P4 has no symmetry, it can also serve as a source of enantiomers. A light-mediated reaction was executed in the presence of S-BINAP as a chiral auxiliary.

A Schlenk tube equipped with a magnetic stirring bar was charged with P4 (0.102 mmol, 50 mg). Distilled methanol (4 mL) was then added to the reaction mixture. The light-mediated reaction was conducted at room temperature for an initial period of 30 minutes, during which the colour of the precursor was observed to change from yellow to reddish brown. Following this initial reaction period, S-BINAP (0.102 mmol, 64 mg) was added to the reaction mixture, and the reaction was allowed to proceed for 24 hours under a nitrogen atmosphere. After completion of the reaction, a

clear greenish-yellow solution was obtained. The mixture was then transferred to a vial, and methanol was added to facilitate dissolution. The Deccan process was employed, and the resulting precipitate was subjected to vacuum drying. Afterward, the product was submitted for NMR analysis, but the desired product was not obtained, as confirmed by NMR spectroscopy.

2.5.6 Synthesis of complex Ru3 and Ru3':

Experimental Procedure:

Following the unsuccessful results, a decision was made to alter **precursor**, with **P1** being selected instead of **P4** A Schlenk tube equipped with a magnetic stirring bar was charged with P1 (0.129 mmol, 50 mg) and R-BINAP (0.387 mmol, 240.97 mg). Distilled methanol (4 mL) was then added to the reaction mixture. The reaction was conducted at reflux temperature (65 °C) for 24 hours under a

nitrogen atmosphere. After that reaction mixture was cooled to room temperature, it was transferred to a vial, and additional methanol was added to facilitate dissolution. The Deccan process was employed, and the resulting precipitate was subjected to vacuum drying. The product was subsequently submitted for LCMS analysis. LCMS (ESI) m/z calculation yielded results for C53H41ClN3P2Ru [M-Cl]⁺ at 918.1513, with 918.44 being found. An additional peak was observed for C53H41ClN3P2ORu [M-Cl]⁺ at 934.1375. The precipitate was filtered and purification via column chromatography using 5% MeOH in DCM was attempted; however, separation of the undesired compound was not achieved. Clear NMR data for this compound was also not obtained.

2.5.7 Synthesis of complex Ru4 and Ru4':

Experimental Procedure:

Following unsuccessful results, a decision was made to first degas the system before S-BINAP was added. A 100 mL two-neck round-bottom for this compound was also not obtained. Dropwise addition of the methanolic solution of S-BINAP was attempted as an alternative to adding it all at once in the same reaction; however, the desired outcome was not achieved in this case either.

2.5.8 Synthesis of complex Ru5 and Ru5':

Experimental Procedure:

After a fruitless result was obtained using precursor P1, a new precursor, P5, which had previously been synthesized in the laboratory, was employed. Due to P5's asymmetric structure, it was identified as a potential source of enantiomers. A 100 mL two-neck round-bottom flask equipped with a magnetic stirring bar was charged with P5 (0.1025 mmol, 41 mg) and dry MeOH (30 ml). For degassing purposes, the reaction mixture was heated at reflux temperature (65 °C). After 1 hour, the mixture was cooled to room temperature. S-BINAP (0.205 mmol, 127.64 mg) was subsequently added, and the reaction was maintained at reflux temperature (65°C) for 24 hours under a nitrogen atmosphere. Upon TLC analysis, S-BINAP was still detected, so the reaction was extended for additional hours. After completion, the reaction mixture was cooled, transferred to a vial, and supplemented with methanol to enhance dissolution. The Deccan process was implemented, and the resulting greenish-yellow precipitate was subjected to vacuum drying. Purification attempts were made via column chromatography using 10% MeOH in EtOAc, with gradual increases in polarity; however, isolation of the desired compound was not accomplished. A colour change to green was observed during chromatography, and enantiomeric separation was not achieved. Clear NMR spectroscopic data for this compound could not be obtained.

2.6.0 Synthesis of complex Ru6 and Ru6':

Experimental Procedure:

As the previous efforts with precursor **P5** proved unproductive, attention was returned to precursor P4, which had previously been synthesized in the laboratory. Due to P4's asymmetric structure, it was identified as a potential source of enantiomers. A Schlenk tube equipped with a magnetic stirring bar was charged with P4 (0.102 mmol, 50 mg), after which distilled methanol (4 mL) was added to the reaction mixture. The light-mediated reaction was conducted at room temperature for an initial period of 30 minutes, during which the colour of the precursor was observed to change from yellow to reddish brown. Subsequently, R-BINAM (0.102 mmol, 64 mg) was added to the reaction mixture, and the reaction was allowed to proceed for 24 hours under a nitrogen atmosphere. Upon TLC analysis after 24 hours, R-BINAM was still detected, so the reaction was extended for additional hours. Following completion, a clear greenish-yellow solution was obtained. The mixture was transferred to a vial, and additional methanol was added to facilitate dissolution. The Deccan process was employed, and the resulting precipitate was subjected to vacuum drying. The product was then submitted for NMR analysis; however, the desired product was not obtained, as confirmed by NMR spectroscopy.

2.6.1 Synthesis of complex Ru7 and Ru7':

Experimental Procedure:

In light of the unsuccessful attempts with precursor **P4**, research efforts were refocused on precursor **P1**, previously synthesized in the laboratory. P1's asymmetric structure was considered advantageous as a potential enantiomer source. A higher temperature approach was implemented for this reaction sequence. A Schlenk tube equipped with a magnetic stirring

bar was charged with **P1** (0.129 mmol, 50 mg) and S-BINAM (0.129 mmol, 36.97 mg). Ethylene glycol (2 mL) was added to the reaction mixture. The reaction was conducted at reflux temperature (190°C) for 4 hours under a nitrogen atmosphere. Following temperature reduction to

ambient conditions, addition of an aqueous KPF6 solution resulted in brown solid precipitation. The precipitate was collected by filtration and purification was attempted via column chromatography using 10% MeOH in EtOAc, with gradual polarity increases. Despite these efforts, the desired compound could not be isolated, and definitive NMR spectroscopic characterization was not achieved.

2.6.2 Synthesis of complex Ru8 and Ru8':

Experimental Procedure:

Following the failed attempts with precursor P1, attention was redirected to precursor **P4**, which had been previously synthesized in the laboratory. 's asymmetric structure was considered advantageous as a potential enantiomer source. A Schlenk tube equipped with a magnetic stirring bar was charged with P4 (0.102 mmol, 50 mg) and S-BINAM (0.102 mmol, 29.23 mg). The same reaction was then performed in two different solvents. First, EtOH (4 ml) was used as a solvent, and second, dry MeOH (4 ml) was employed. The reflux temperature was provided for each solvent, and both reactions were conducted for 24 hours. When EtOH was used as the solvent, results similar to previous reactions were obtained. However, when dry MeOH was used, more favourable outcomes were achieved. After the reaction in dry MeOH was completed, the mixture was allowed to cool to room temperature. Following temperature reduction to ambient conditions, yellow solid precipitation was observed upon addition of an aqueous KPF6 solution. The precipitate was collected by filtration, and purification was attempted via column chromatography using 10% MeOH in EtOAc, with gradual polarity increases.

The desired compound, consisting of two sets of enantiomers, was obtained with an enantiomeric ratio of 3:1; however, the aliphatic region peaks were not clearly resolved. Despite multiple attempts, separation of

these two enantiomers by column chromatography could not be achieved. Nevertheless, it was proven that two sets of diastereomers are present in the system, as confirmed by NMR spectroscopy.

CHAPTER 3

RESULTS AND DISCUSSION

3.1 Synthesis of Ligands:

The suitable ligand L1 and ligand precursor salt L1.HI have been synthesized with 75% (scheme 1) and 86% yield. 1 H NMR data confirmed the existence of this compound (L1.HI) by giving the resonance at δ 10.26 (s) for the imidazole proton of the carbene groups and δ 8.39 (t) for pyridine proton. (Scheme 2)

Ligand L2 have been synthesized by treating with 2-bromopyridine and imidazole and then K₂CO₃ was added to obtain a yellowish-white solid; 95%.

L3 and L4 have been synthesized by treating L2 with MeI/ ⁱPrI and then toluene was added to obtain **yellow solids L3 (80.8% yield)** and **L4 (62.76% yield)**, respectively. ¹H NMR data confirmed the existence of the compound L3 as well as L4 by giving the resonance at δ 10.72 (s) for imidazole proton in case of L3 and δ 1.57 (d) for isopropyl substituted imidazole protons in case of L4. (**Scheme 3**)

$$\begin{array}{c|c} & & & \\ Br & N & Br & N \\ \hline \end{array} \xrightarrow{\begin{subarray}{c} H \\ N \\ \hline \end{array}} \xrightarrow{\begin{subarray}{c} K_2CO_3, Cul, DMSO, TEMED \\ 120 °C, 24h \\ \hline \end{array} \xrightarrow{\begin{subarray}{c} N \\ N \\ \hline \end{array}} \xrightarrow{\begin{subarray}{c} N \\ N \\ \end{array}} \xrightarrow{\begin{subarray}{c} N \\ N \\ \end{array}$$
}

Scheme 1: Synthesis of Ligand L1

Scheme 2: Synthesis of Ligand L1.HI

Scheme 3: Synthesis of Ligand L3 and L4 from L2

3.2 Synthesis of Precursor P1 and P2:

To synthesize the complex Precursor P1 and P2, individually treating L3 with RuCl₃.3H₂O in THF for Precursor P1 and similarly L4 with RuCl₃.3H₂O in THF for Precursor P2 to obtain brown solids P1 (68.8% yield) and P2 (61.15% yield), respectively. Both this complex was characterized by mass spectrometry. (LCMS (ESI) found 348.93 [M–Cl] $^+$, 366.94 [M–Cl+H₂O] $^+$; UV-vis λ_{max} /CH₃CN for the P1 is 384 nm and (LCMS (ESI) found 376.96 [M–Cl] $^+$; UV-vis λ_{max} /CH₃CN for the P2 (2b is 385 nm) (**Scheme 5**)

Scheme 4: Synthesis of Ligand P1 and P2

3.3 Synthesis of Precursor P3:

Again for the synthesis of P3 the pincer ligand precursor L1.HI and Ruthenium precursor Ru1 (2a) were taken and refluxed in ethylene glycol conditions followed by saturated solutions of KPF₆ was added to obtain a yellowish-orange solid identified as Ru-3a **60.06%** (200 mg). The complex was characterized using 1 H, 13 C, and 31 P NMR spectroscopy. In the 1 H NMR spectrum recorded in DMSO-d6, two distinct species were observed in solution: P3 (58%) with a doublet at δ 12.96, and P3' (42%) with a doublet at δ 12.28. This phenomenon arises from the substitution of iodide by the nucleophilic DMSO solvent, resulting in two separate signals for the same ortho proton of the pyridine ring. (Scheme 5)

Scheme 5: Synthesis of precursor P3

3.4 Synthesis of precursor P4:

For the synthesis of Precursor P4, P1 was treated with DMSO for 3 days at room temperature to obtain a yellow solid in 53% yield (0.091 g). This complex was characterized by mass spectrometry LCMS (ESI) m/z calculated for [M-Cl-DMSO+H₂O]⁺ 391.36 found: 391.97, C₁₃H₂₁N₃O₂RuS₂ [M-2Cl+H]⁺ 416.04 found: 416.00. In the ¹H NMR analysis of **P4**, the signal for the –CH₃ protons was obtained at 4.16 ppm, while the most deshielded peak for the ortho proton of the pyridine ring appeared at 9.47 ppm. (**Scheme 6**)

$$\begin{array}{c|c} CI & N & DMSO \\ H_2O - Ru & & 3 \text{ days, rt} \end{array}$$

$$\begin{array}{c|c} CI & N & \\ \end{array}$$

$$\begin{array}{c|c} (P4) & \\ Yield = 53\% \\ S = DMSO \end{array}$$

Scheme 6: Synthesis of precursor P4

3.5 Synthesis of Precursor P5:

To synthesize precursor P5, compound P1 was dissolved in 2–3 mL of methanol (MeOH), followed by the addition of an excess amount of dimethyl sulfide (1 mL). The reaction mixture was then refluxed for 6 hours. Upon completion, a clear solution was obtained. The solvent was removed by trituration with 20 mL of diethyl ether, leading to the precipitation of the solid product. The resulting solid was collected and dried under vacuum.P5: Yield = 0.056 g (0.123 mmol, 47.4%). LCMS: 419.99 [M-Cl]⁺

Scheme 7: Synthesis of precursor P5

3.6 Synthesis of complexes:

3.6.1 Synthesis of complexesRu1 and Ru1':

The synthesis of two sets of diastereomers, designated as Ru1 and Ru1', was attempted using camphor sulfonate as a chiral auxiliary, with P3 being utilized as the starting precursor. Various methodologies were

implemented, including the application of different solvents and the establishment of diverse suitable conditions; however, the desired product could not be obtained. The silver salt of camphor sulfonate was also employed, but the intended result was not achieved. Furthermore, ion exchange with an aqueous solution of camphor sulfonate was attempted, which similarly failed to yield the desired outcome. Despite multiple methodological variations being explored, the approach to separate diastereomeric pairs was unsuccessful, as evidenced by LCMS (ESI) analysis, wherein the calculated m/z value of 717.1548 for [M-PF₆]⁺ was not detected.

Scheme 8: Synthesis of complex Ru1 and Ru1'

3.6.2 Synthesis of complex Ru2 and Ru2':

Following unsuccessful results with precursor P3, new diastereomers Ru2 and Ru2' were trying to synthesize using precursor P4 and S-BINAP as achiral auxiliary instead of camphor sulfonate. P4 was dissolved in distilled MeOH (4ml), and a light-mediated reaction was conducted at room temperature. A colour change from yellow to reddish brown was observed during the initial 30-minute period. S-BINAP was then added, and the reaction was continued for 24 hours under nitrogen atmosphere. Upon completion, a greenish-yellow

solution was obtained after aqueous KPF₆ addition. LCMS (ESI) analysis revealed m/z values of 918.44 (calculated: 918.1513) for C₅₃H₄₁ClN₃P₂Ru [M-Cl]⁺ and an additional peak at 934.1375 for C₅₃H₄₁ClN₃P₂ORu [M-Cl]⁺. Although purification via column chromatography using 5% MeOH in DCM was attempted, separation of the undesired compound was not achieved, and clear NMR data could not be obtained.

Scheme 9: Synthesis of complex Ru2 and Ru2'

3.6.3 Synthesis of complex Ru3 and Ru3':

As the previous efforts with precursor P4 proved unproductive, a change in the precursor was implemented with P1 being selected instead of P4. P4 and R-BINAP were dissolved in dry methanol (4 ml), and the reaction was conducted at reflux temperature (65 °C) for 24 hours under a nitrogen atmosphere. The Deccan process was employed, and the resulting precipitate was subjected to vacuum drying. By LCMS (ESI) analysis, an m/z value of 918.44 was found for C₅₃H₄₁ClN₃P₂Ru [M-Cl]⁺ (calculated: 918.1513), along with an additional peak of higher intensity at 934.1375 for C53H41ClN3P2ORu [M-Cl]+. After filtration of the precipitate, purification was attempted via column chromatography using 5% MeOH in DCM; however, the undesired compound could not be separated, and clear NMR data could not be obtained.

Scheme 10: Synthesis of complex Ru3 and Ru3'

3.6.4 Synthesis of complex Ru4 and Ru4':

Following negative results, a system degassing approach was implemented prior to S-BINAP addition. Dry MeOH (30 ml) was used to dissolve P1, and the reaction mixture was heated at methanol's reflux temperature (65 °C) for degassing purposes. After cooling to room temperature, S-BINAP was introduced, and the reaction was continued at reflux temperature for 24 hours under nitrogen atmosphere. A greenish-brown precipitate was obtained via the Deccan process and was subjected to vacuum drying. Purification was attempted through column chromatography using 10% EtOAc in DCM; however, the desired compound could not be separated. A colour change to green was observed during chromatography, and diastereomeric separation was not achieved. Structure of the expected complexes couldn't be interpreted from the NMR data. An alternative approach involving dropwise addition of methanolic S-BINAP solution was also attempted, but the desired outcome remained unattained.

Scheme 11: Synthesis of complex Ru4 and Ru4'

3.6.5 Synthesis of complex Ru5 and Ru5':

Following fruitless results with precursor P1, precursor P5 was employed as a replacement. P5 was dissolved in dry MeOH (30 ml), and the reaction mixture was heated at reflux temperature (65 °C) for degassing purposes. After being cooled to room temperature, S-BINAP was added, and the reaction was maintained at reflux temperature for 24 hours under nitrogen atmosphere. When S-BINAP was still detected by TLC analysis, the reaction was extended for additional hours. A greenish-yellow precipitate was obtained via the Deccan process and was subjected to vacuum drying. Purification was attempted through column chromatography using 10% MeOH in EtOAc with gradual increases in polarity; however, the desired compound could not be isolated. A colour change to green was observed during chromatography, and diastereomeric separation was not achieved. Clear NMR spectroscopic data could not be obtained for this compound.

Scheme 12: Synthesis of complex Ru5 and Ru5'

3.6.6 Synthesis of complex Ru6 and Ru6':

Following unproductive efforts with precursor P5, attention was redirected to precursor P4. P4 was dissolved in distilled MeOH, and a light-mediated reaction was conducted at room temperature for 30 minutes, during which a colour change from yellow to reddish brown was observed. S-BINAM was employed as a new chiral auxiliary instead of S-BINAP, and the reaction was maintained under a nitrogen atmosphere for 24 hours. After TLC analysis revealed the continued presence of S-BINAM, the reaction duration was extended. Upon completion, a greenish-yellow solution was obtained

following aqueous KPF₆ addition. The desired product was not detected, as confirmed by NMR spectroscopy, where botharomatic and aliphatic region peaks were not clearly observed. Additionally, S-BINAM dissociation was evident from its peaks in the NMR spectrum.

Scheme 13: Synthesis of complex Ru6 and Ru6'

3.6.7 Synthesis of complex Ru7 and Ru7':

Due to unsuccessful attempts with precursor P4, research efforts were redirected to precursor P1. P1 and S-BINAM were dissolved in ethylene glycol (2 mL), and the reaction was conducted at reflux temperature (190 °C) for 4 hours under a nitrogen atmosphere. After the temperature was reduced to ambient conditions, brown solid was precipitated by the addition of an aqueous KPF6 solution. The precipitate was collected by filtration, and purification was attempted via column chromatography using 10% MeOH in EtOAc with gradual polarity increases. Despite these efforts, isolation of the desired compound could not be achieved, and definitive NMR spectroscopic characterization was not obtained. Structure of the expected complexes couldn't be interpreted from the NMR data.

Scheme 14: Synthesis of complex Ru7 and Ru7'

3.6.8 Synthesis of complex Ru8 and Ru8':

Following failed attempts with precursor P1, attention was redirected to precursor P4. P4 and S-BINAM were dissolved in two different solvents: EtOH (4 ml) and dry MeOH (4 ml). Both reactions were conducted at reflux temperature for 24 hours. When EtOH was used, results similar to previous reactions were obtained. However, when dry MeOH was used, more favourable outcomes were achieved. After cooling to ambient conditions, yellow solid was precipitated by the addition of an aqueous KPF₆ solution. The precipitate was collected by filtration, and purification was attempted via column chromatography using 10% MeOH in EtOAc with gradual polarity increases. Two sets of diastereomers were obtained with a diastereomeric ratio of 3:1, as evidenced by NMR spectroscopy showing two distinct signals: for the pyridine ortho proton (doublets at δ 9.45 for Ru8 and δ 9.39 for Ru8') and for the imidazole proton (singlets at δ 7.09 for Ru8 and δ 7.07). However, the aliphatic region peaks were not clearly resolved, and S-BINAM proton signals were also observed in the spectra. Despite multiple attempts, separation of these diastereomers by column chromatography could not be achieved, although their presence in the system was confirmed by NMR analysis.

Scheme 15: Synthesis of complex Ru8 and Ru8'

3.7.1 Characterization of Ligand L1.HI

3.7.1.1 LCMS of Ligand L1.HI

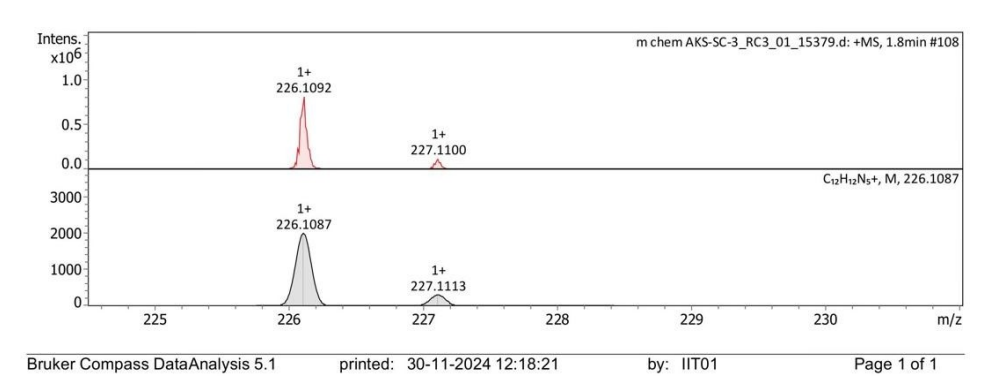


Fig.7: LCMS of L1.HI

3.7.1.2 NMR spectra of Ligand L1.HI

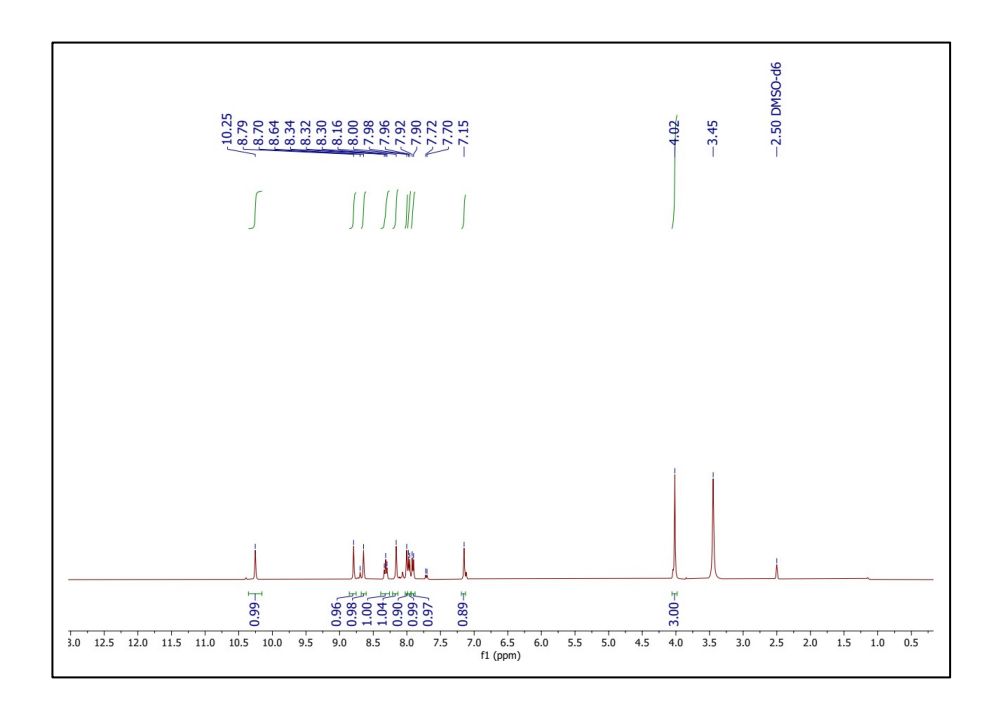


Fig.8: ¹H NMR of Ligand L1.HI in DMSO-d₆

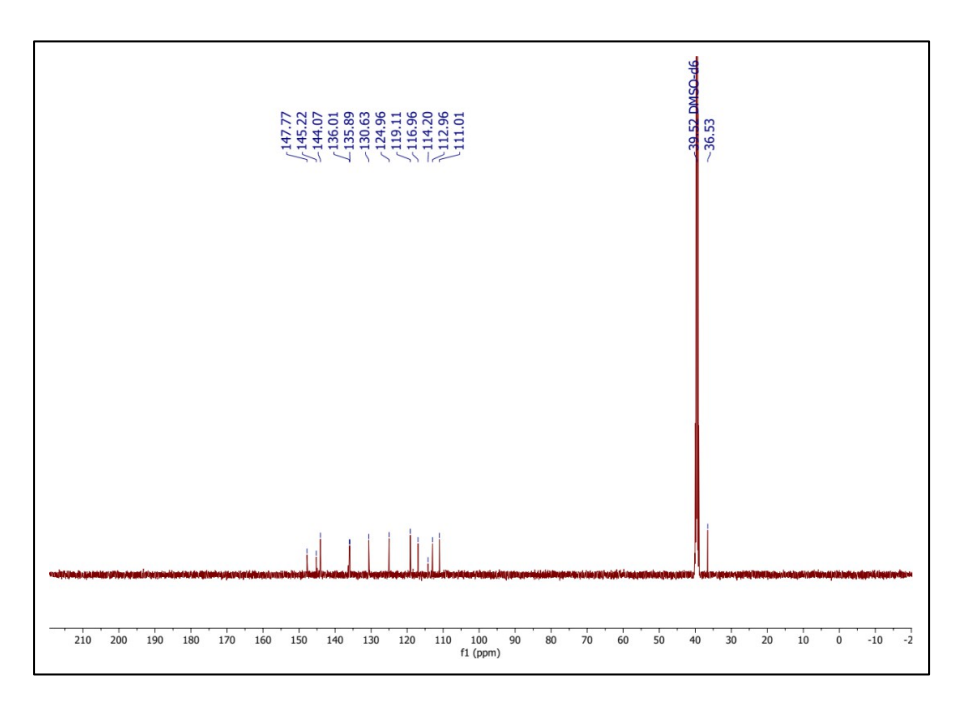


Fig.9: ¹³C{¹H} NMR of Ligand L1.HI in DMSO-d₆

3.7.2 Characterization of Ligand L2

3.7.2.1 LCMS of Ligand L2

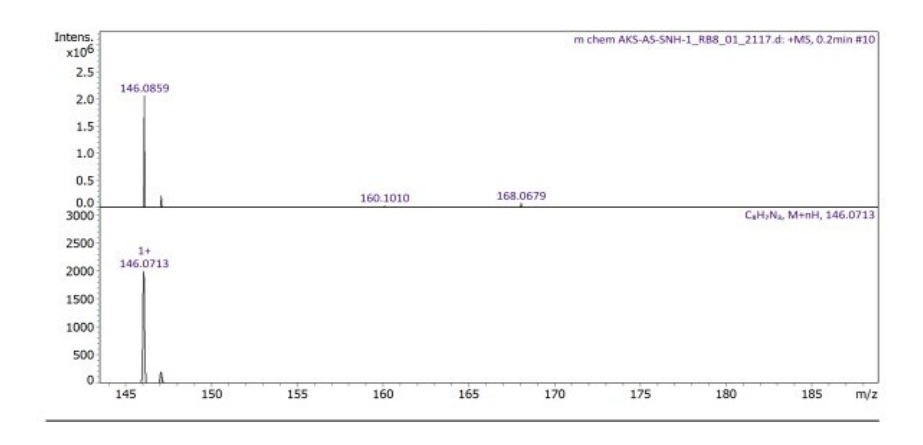


Fig.10: LCMS of L2

3.7.3 Characterization of Ligand L3

3.7.3.1 LCMS of Ligand L3

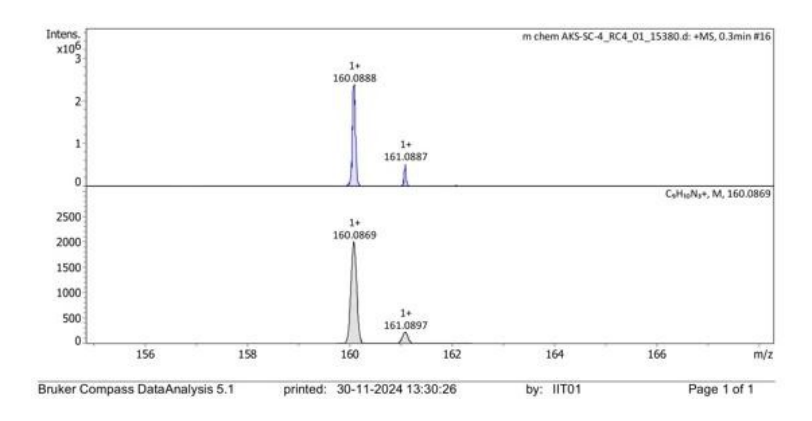


Fig.11: LCMS of L3

3.7.3.2 NMR spectra of Ligand L3

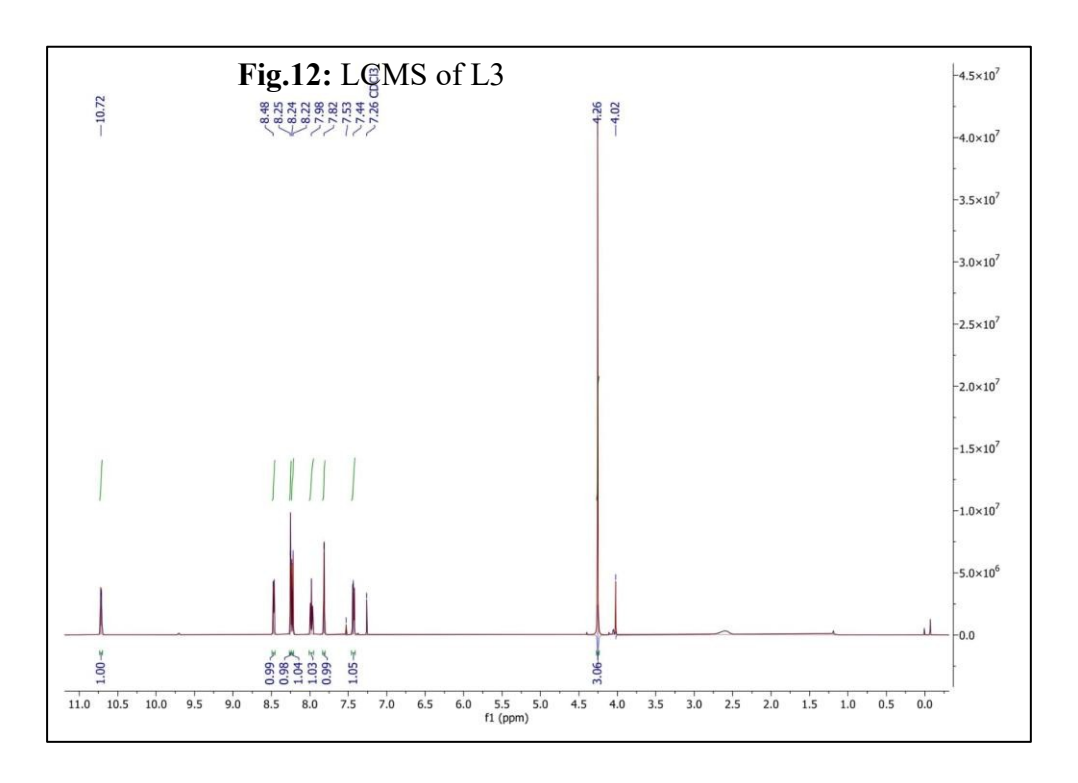


Fig.12:1H NMR spectrum of L3 in CDCl₃

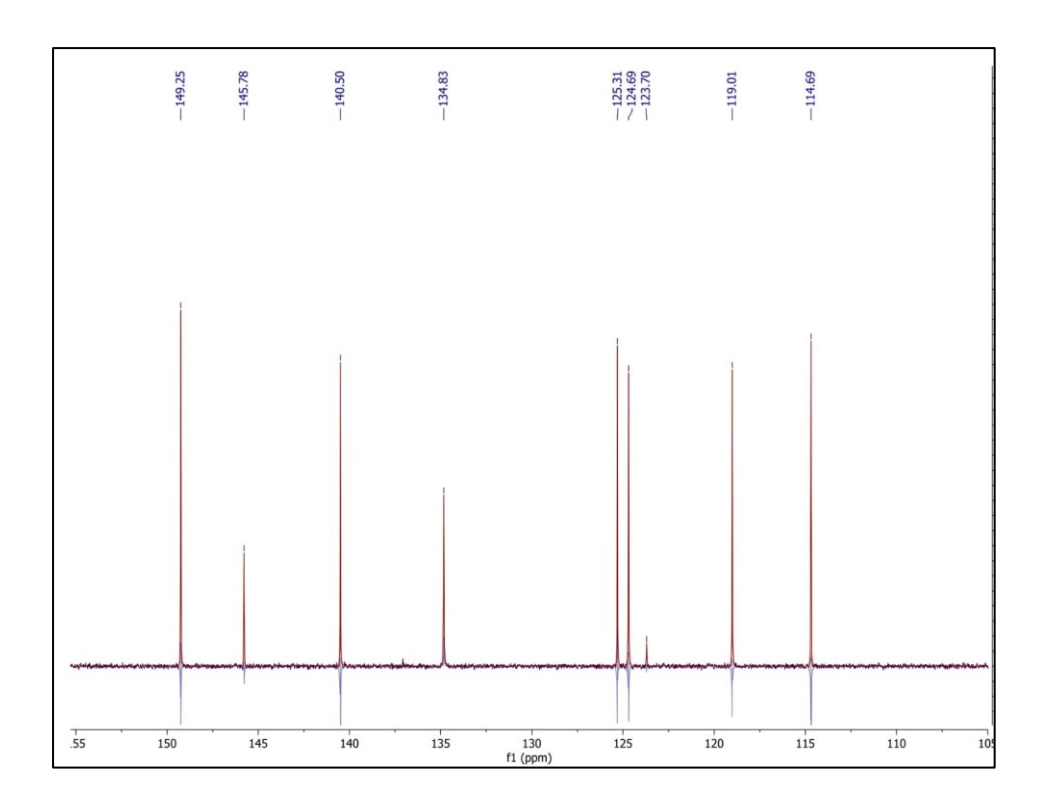


Fig.13: ${}^{13}C\{{}^{1}H\}$ spectrum of L3 in CDCl₃

3.7.4 Characterization of Ligand L4

3.7.4.1 LCMS of Ligand L4

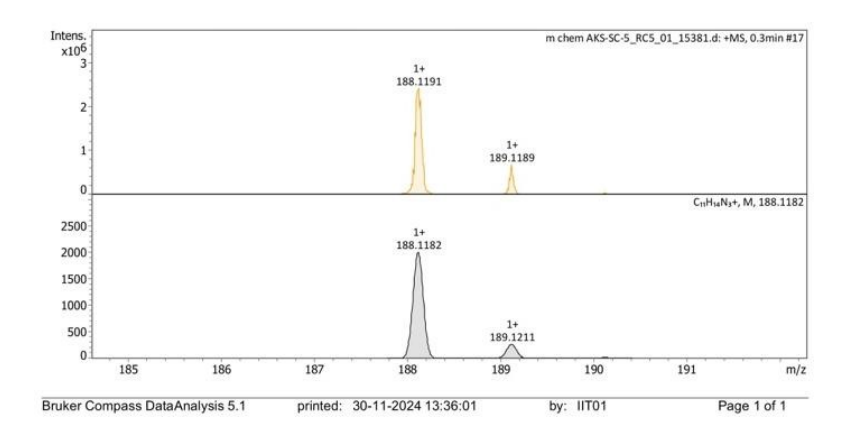


Fig.14: LCMS of Ligand L4

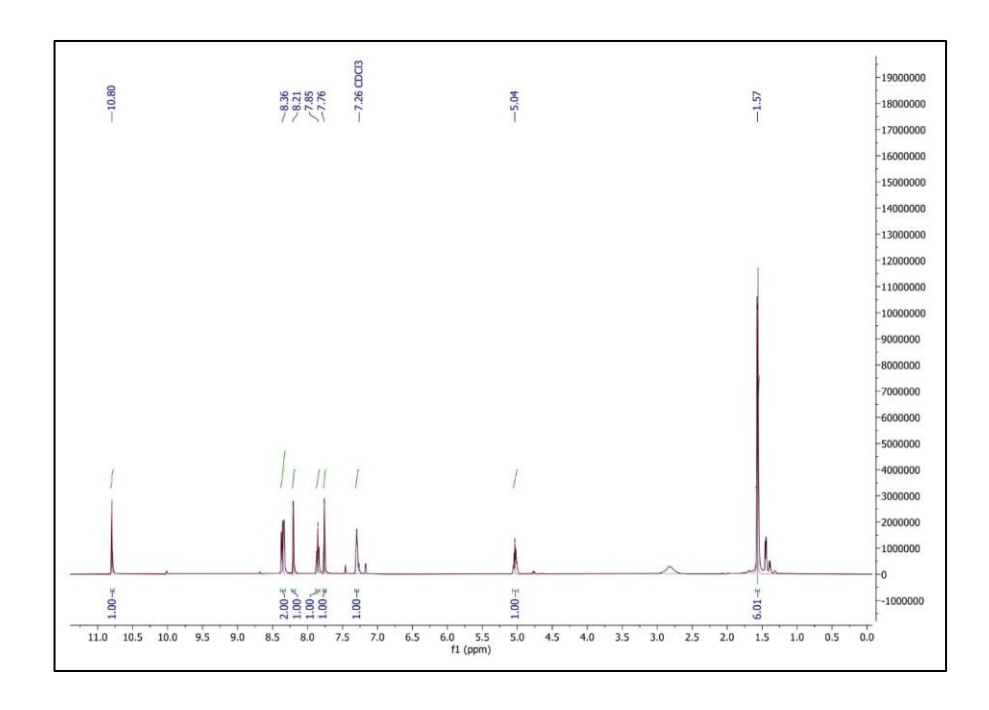


Fig.15: ¹H NMR spectrum of L4 in CDCl₃

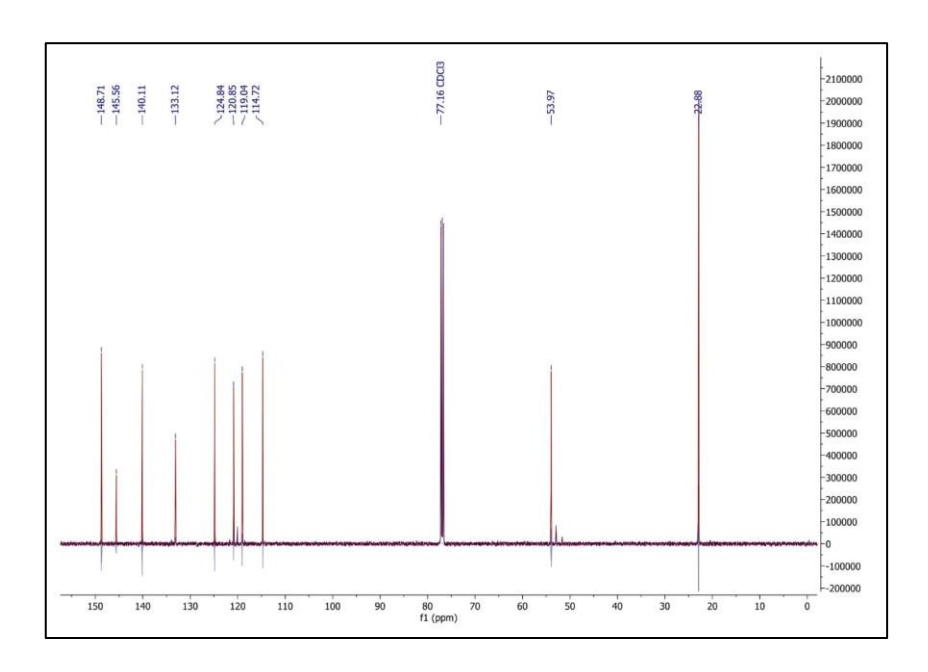


Fig.16: ¹³C{¹H} NMR spectrum of L4 in CDCl₃

3.7.5 Characterization of Precursor P1

3.7.5.1 LCMS of Precursor P1

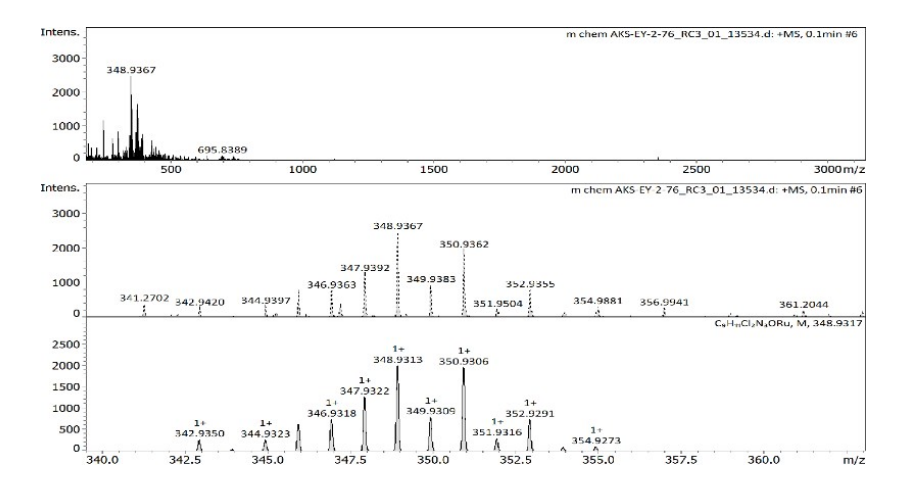


Fig.17: LCMS of Precursor P1

3.7.5.2 UV-Vis spectra of Precursor P1

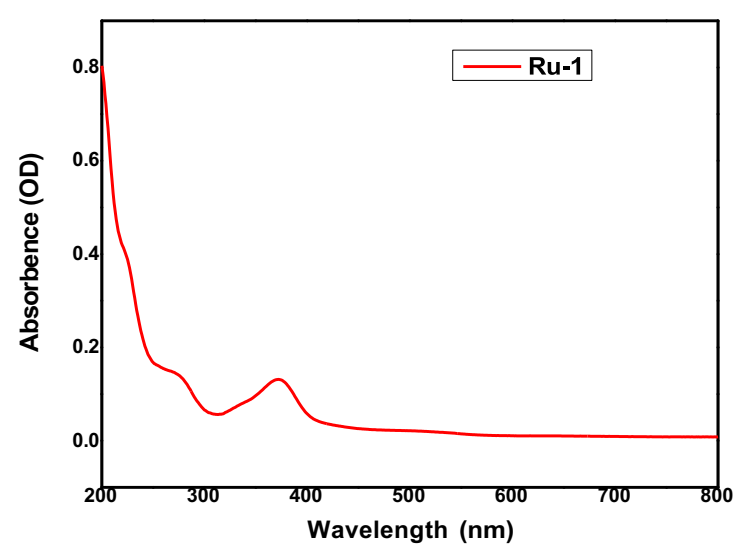


Fig.18: UV-Vis spectra of Precursor P1

3.7.6 Characterization of Precursor P2

3.7.6.1 LCMS of Precursor P2

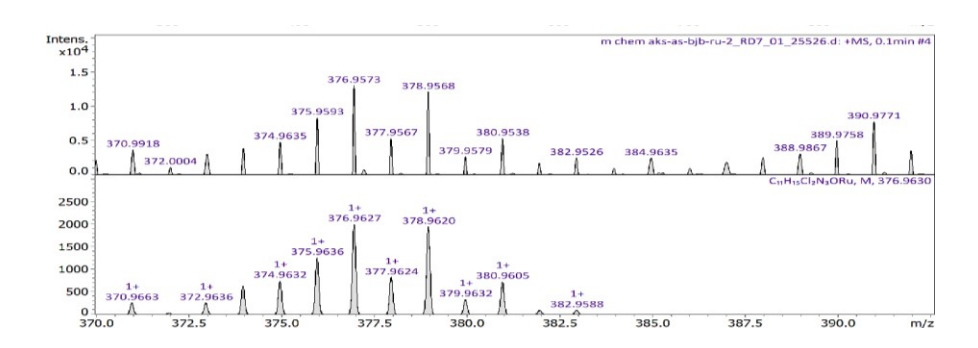


Fig.19: LCMS of Precursor P2

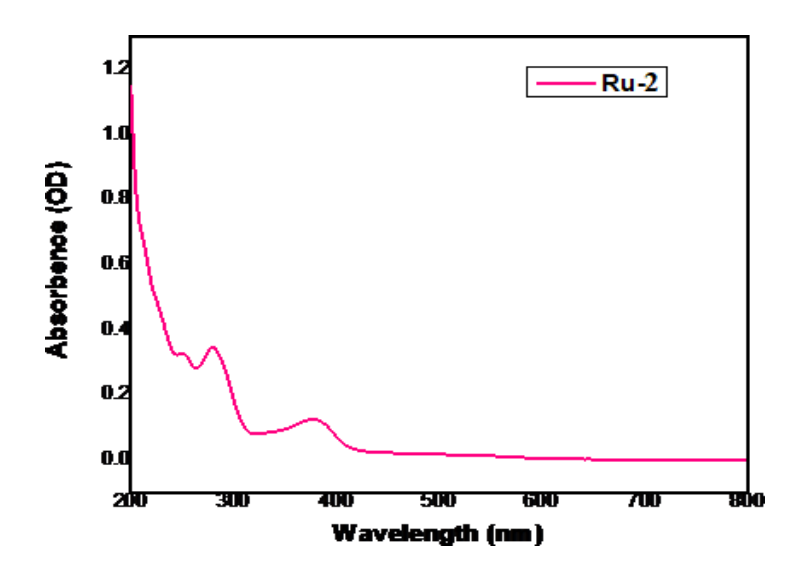


Fig.20: UV-Vis spectra of Precursor P2

3.7.7 Characterization of Precursor P3

3.7.7.1 NMR spectra of **Precursor P3**

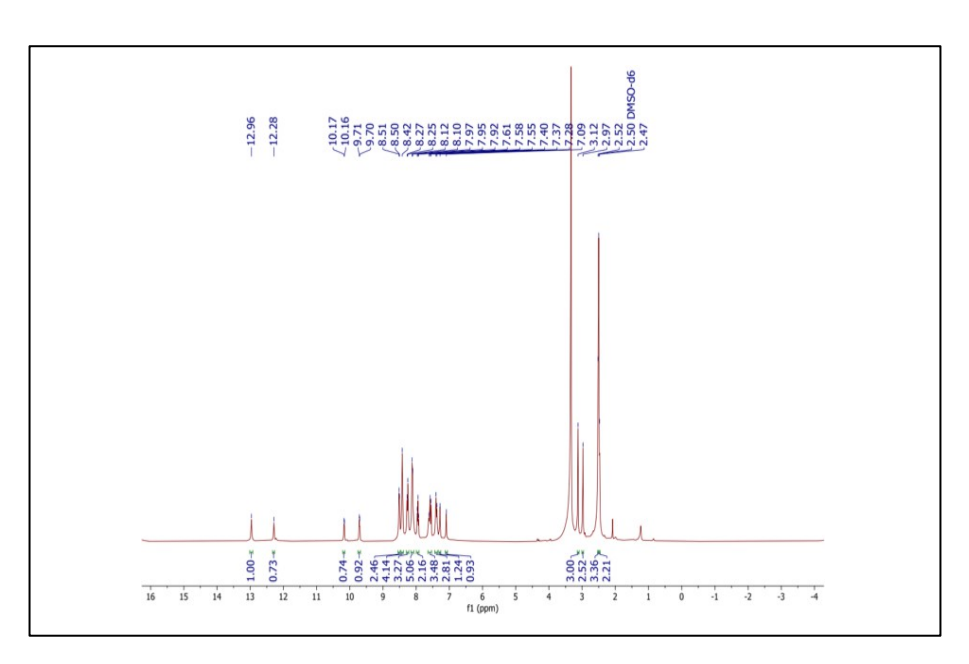


Fig.21: ¹H NMR of Precursor P3 in DMSO-d₆

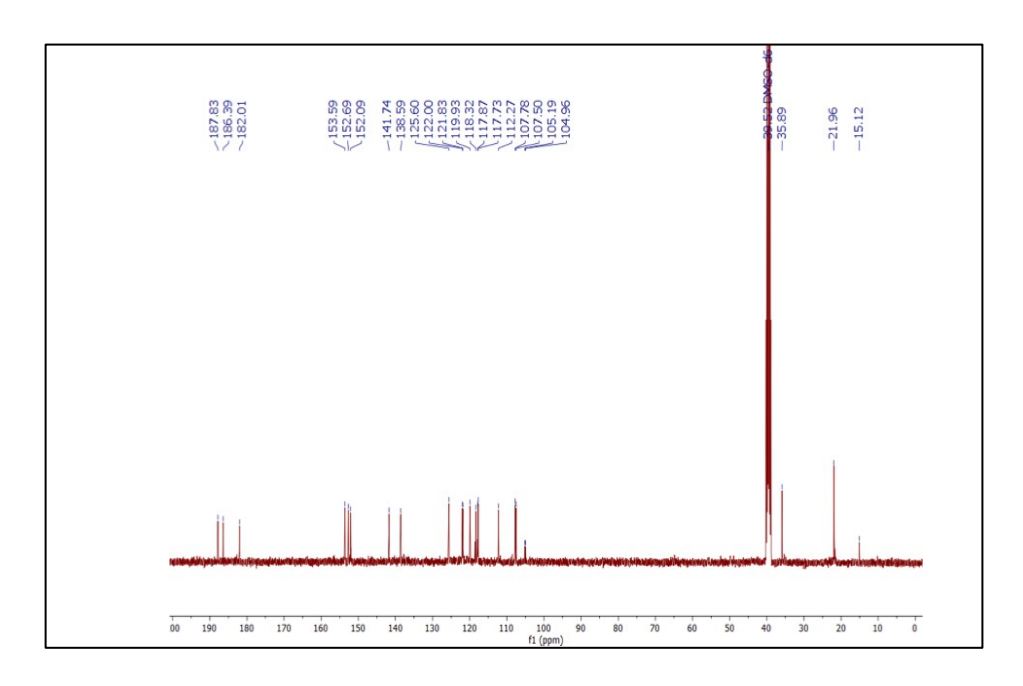


Fig.22: ¹³C{¹H} NMR of Precursor P3 in DMSO-d₆

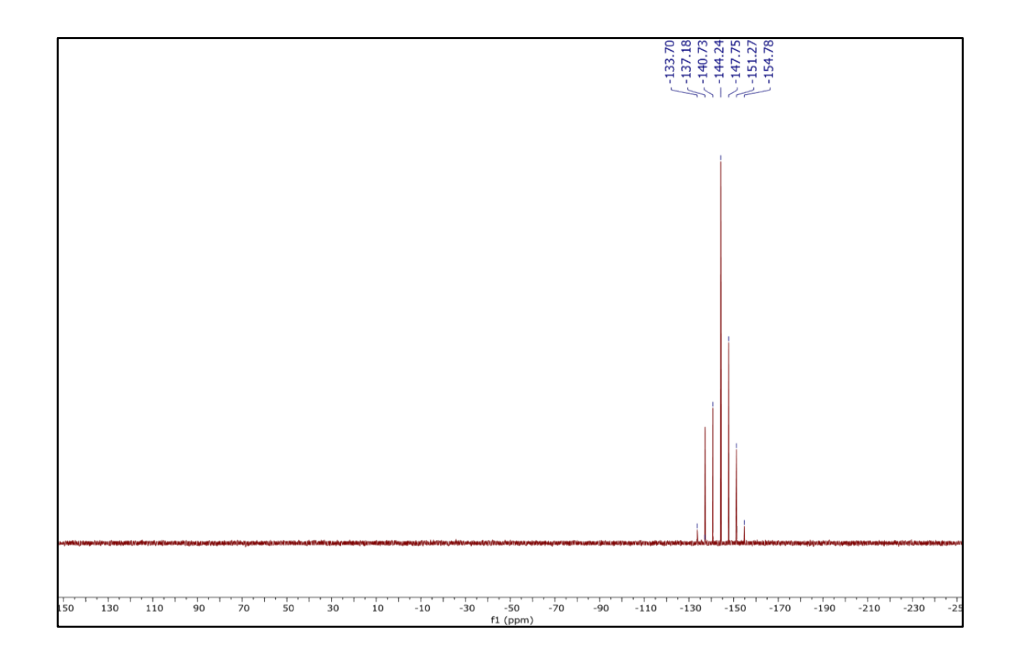


Fig.23: ³¹P{¹H} NMR of Precursor P3 in DMSO-d₆

3.7.8 Characterization of Precursor P4

3.7.8.1 LCMS of Precursor P4

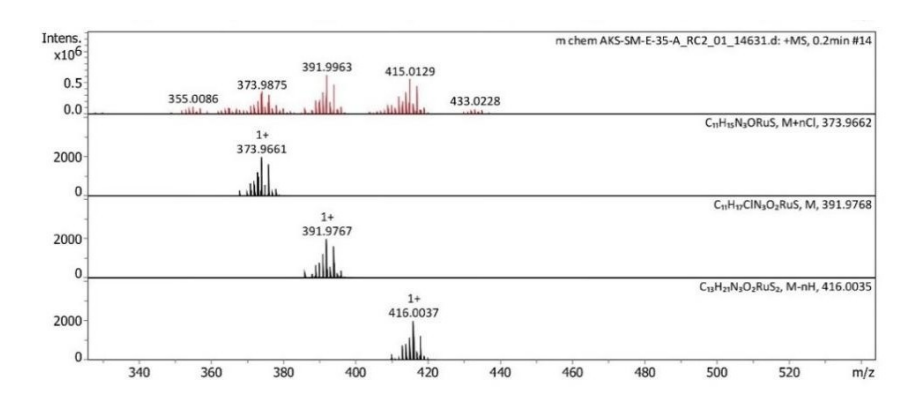


Fig.24: LCMS of Precursor P4

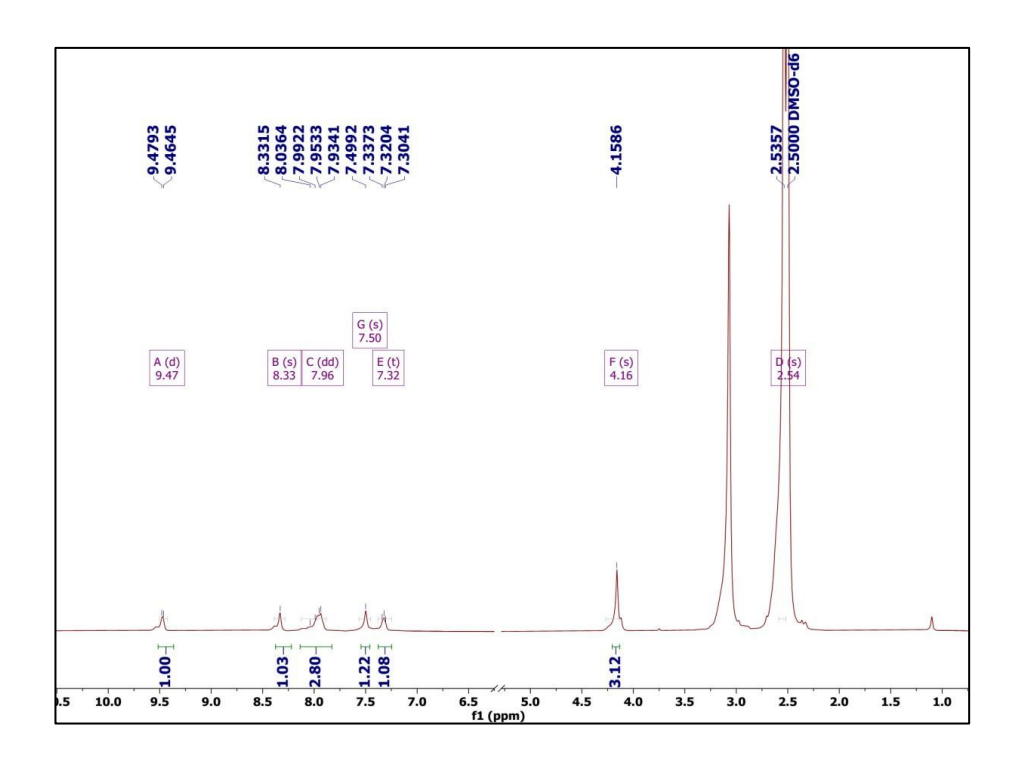


Fig.25: ¹H NMR of Precursor P4 in DMSO-d₆

3.7.9 Characterization of Precursor P5

3.7.9.1 LCMS of Precursor P5

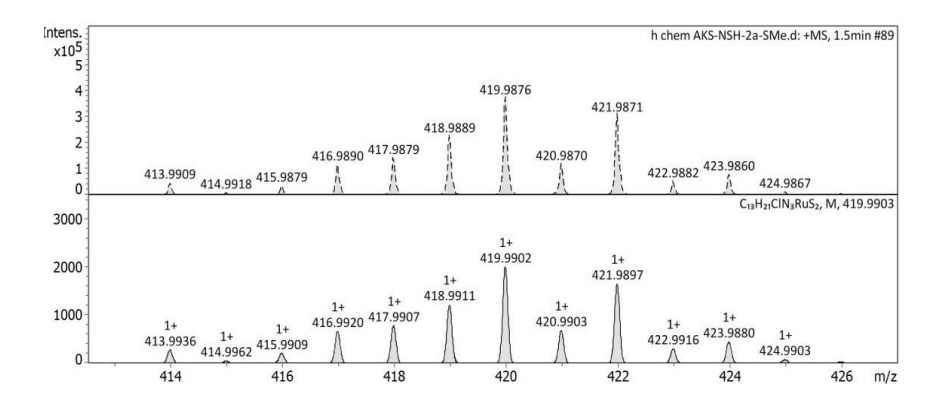


Fig.26: LCMS of Precursor P5

3.8.0 Characterization of complex Ru1 and Ru1':

3.8.1.1 LCMS of Complex Ru1 and Ru1'

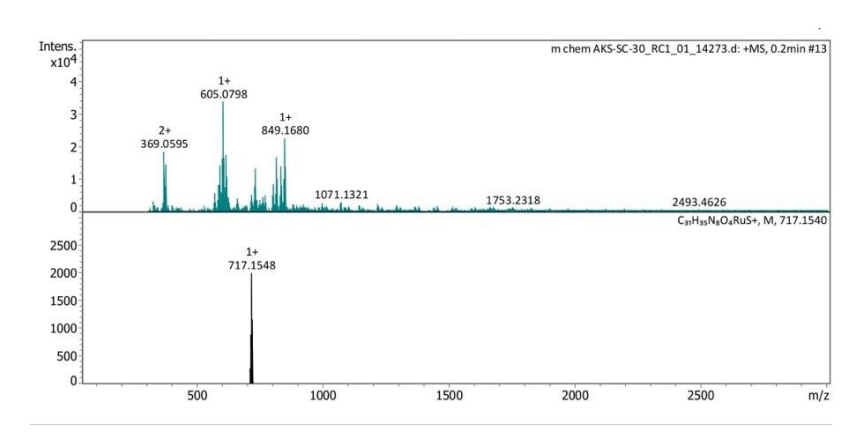


Fig 27 a. The expected product is not obtained, as confirmed by LCMS (LCMS (ESI) m/z calculated for [M-PF₆] 717.1548)

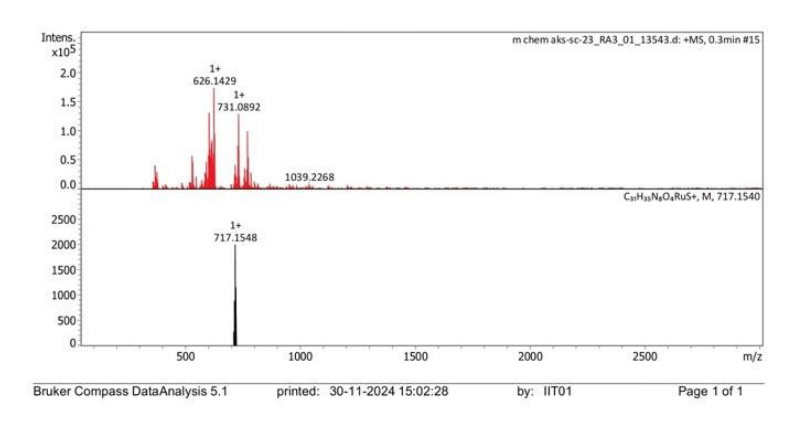


Fig 27 b. The expected product is not obtained, as confirmed by LCMS (LCMS (ESI) m/z calculated for [M-PF₆] 717.1548)

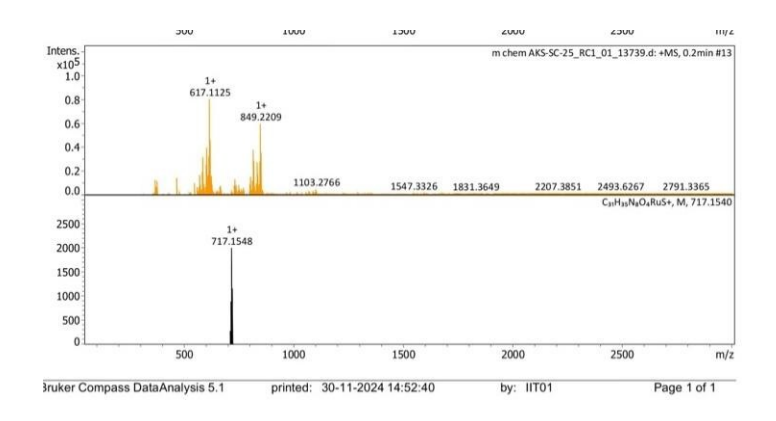


Fig 27 c. The expected product is not obtained, as confirmed by LCMS (LCMS (ESI) m/z calculated for $[M-PF_6]$ 717.1548)

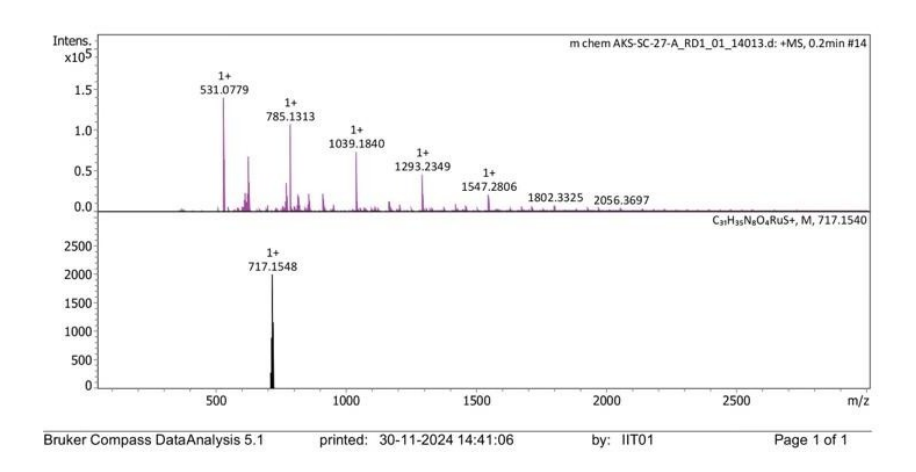


Fig 27 d. The expected product is not obtained, as confirmed by LCMS (LCMS (ESI) m/z calculated for [M-PF₆]

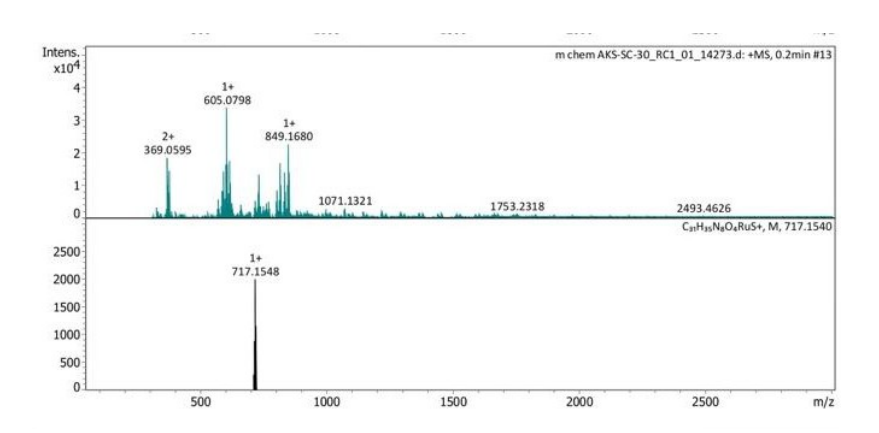


Fig 27 e. The expected product is not obtained, as confirmed by LCMS (LCMS (ESI) m/z calculated for [M-PF₆] 717.1548)

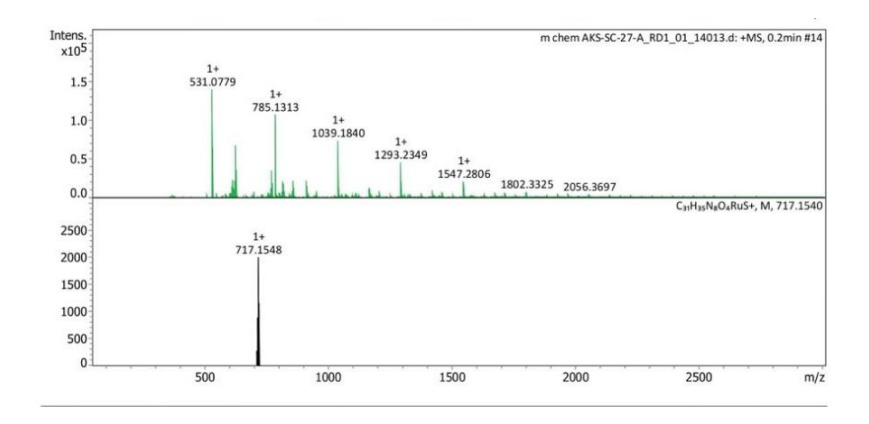


Fig 27 f. The expected product is not obtained, as confirmed by LCMS (LCMS (ESI) m/z calculated for [M-PF₆] 717.1548)

3.8.2 Characterization of complex Ru2 and Ru2':

3.8.2.1 LCMS of Complex Ru2 and Ru2'

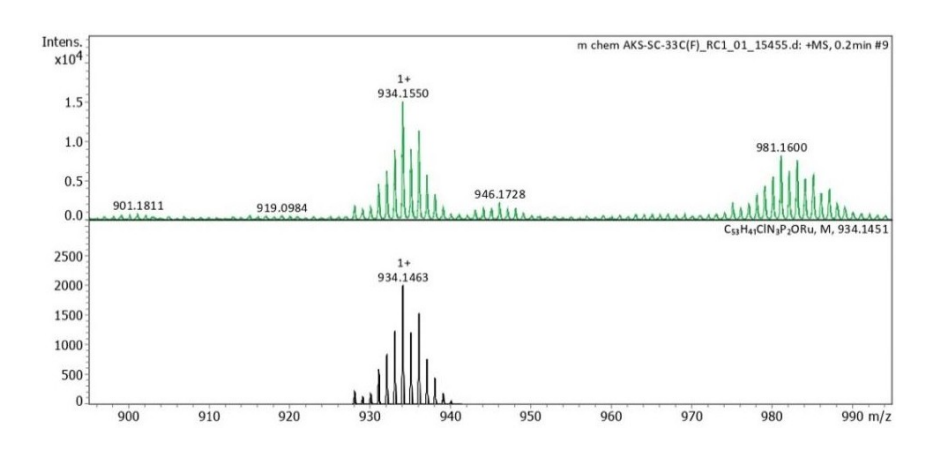


Fig 28. An additional peak is obtained as confirmed by LCMS (LCMS (ESI) m/z calculated for $C_{53}H_{41}ClN_3P_2ORu$ [M-Cl]⁺ 934.1375

3.8.3 Characterization of complex Ru3 and Ru3':

3.8.3.1 LCMS of Complex Ru3 and Ru3'

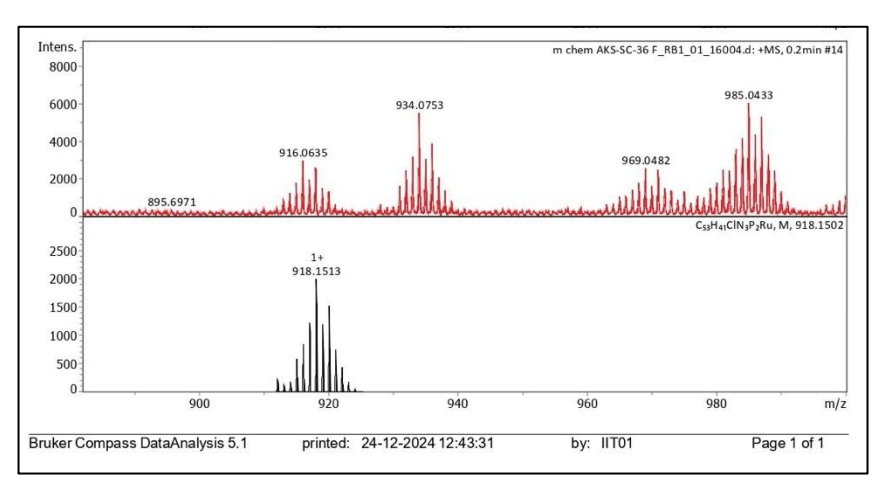


Fig 29. An additional peak is obtained as confirmed by LCMS (LCMS (ESI) m/z calculated for $C_{53}H_{41}ClN_3P_2ORu$ [M-Cl]⁺ 934.1375

3.8.4 Characterization of complex Ru4 and Ru4':

3.8.4.1 NMR spectra of complex Ru4 and Ru4'

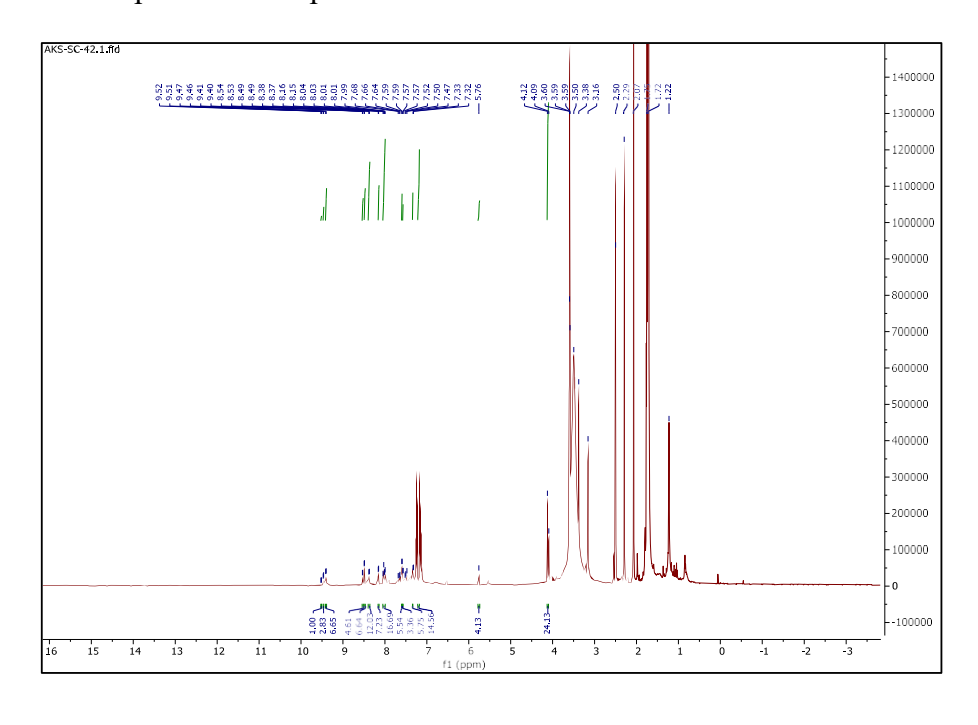


Fig30. ¹H NMR spectra of Ru4 and Ru4'

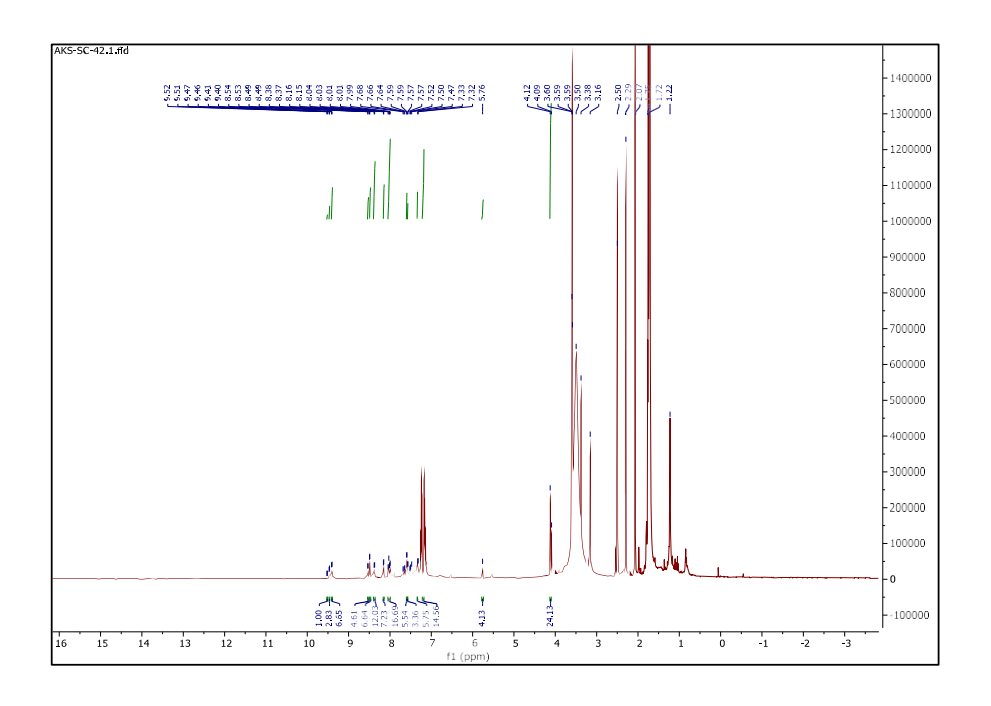


Fig31. $^{13}C\{^{1}H\}$ NMR spectra of Ru4 and Ru4'

3.8.5 Characterization of complex Ru5 and Ru5':

3.8.5.1 NMR spectra of complex Ru5 and Ru5'

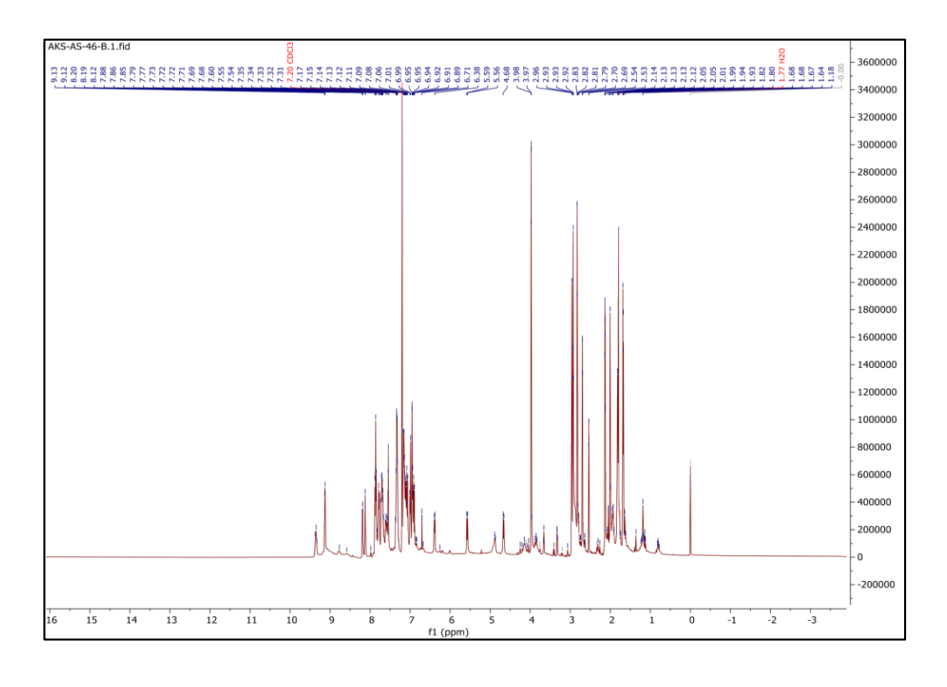


Fig32. ¹H NMR spectra of Ru5 and Ru5'

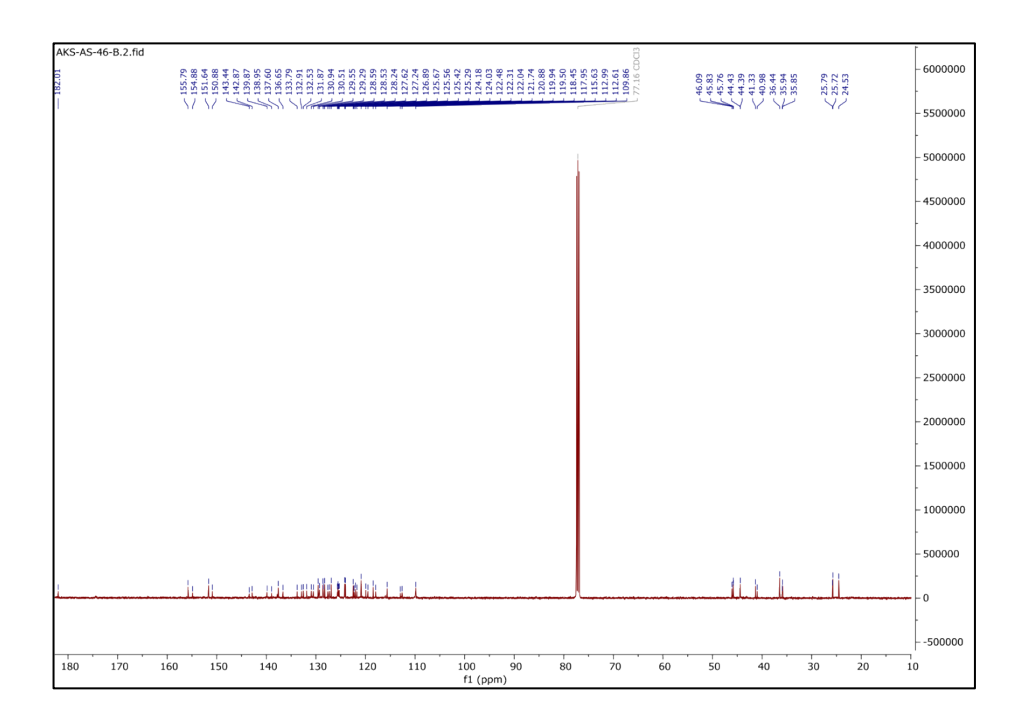


Fig33. $^{13}C\{^{1}H\}$ NMR spectra of Ru5 and Ru5'

3.8.6 Characterization of complex Ru6 and Ru6':

3.8.6.1 NMR spectra of complex Ru6 and Ru6'

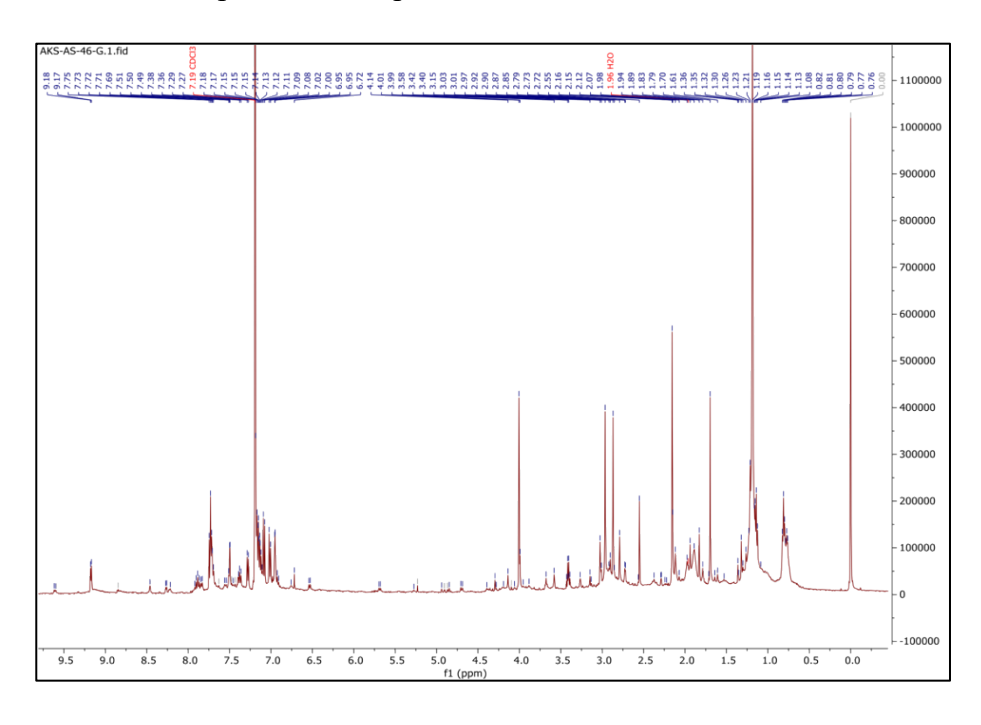


Fig34. ¹H NMR spectra of Ru6 and Ru6'

3.8.7 Characterization of complex Ru7 and Ru7':

3.8.7.1 NMR spectra of complex Ru7 and Ru7'

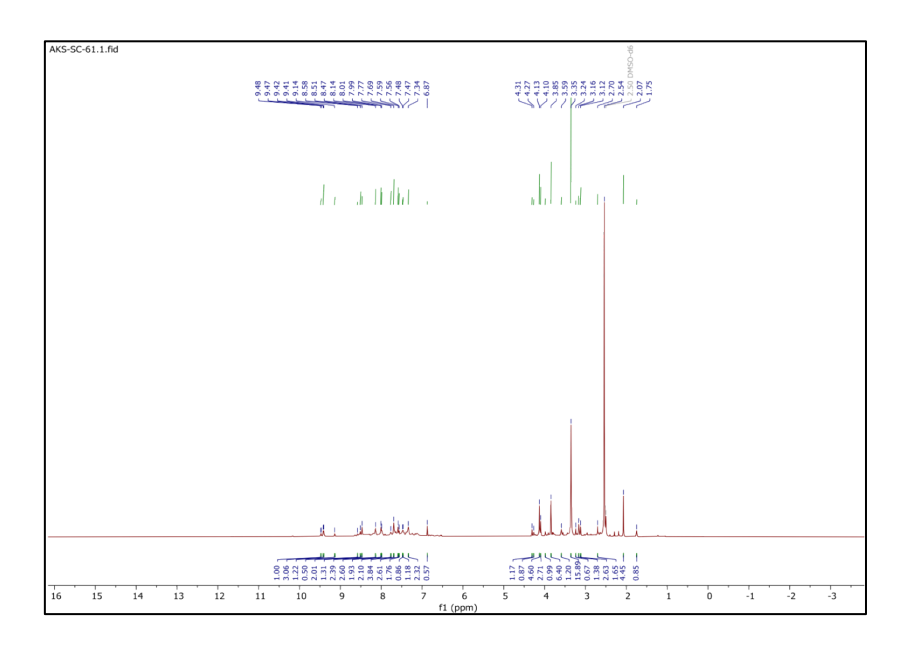


Fig35. ¹H NMR spectra of Ru7 and Ru7'

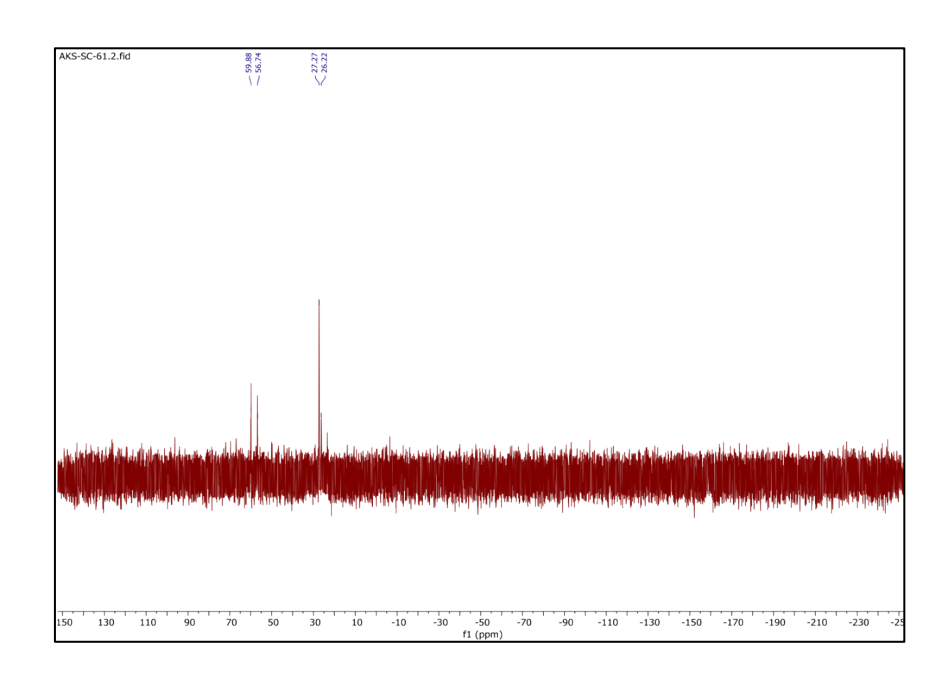


Fig36. ¹³C{¹H} NMR spectra of Ru and Ru7'

3.8.8 Characterization of complex Ru8 and Ru8':

3.8.8.1 NMR spectra of complex Ru8 and Ru8'

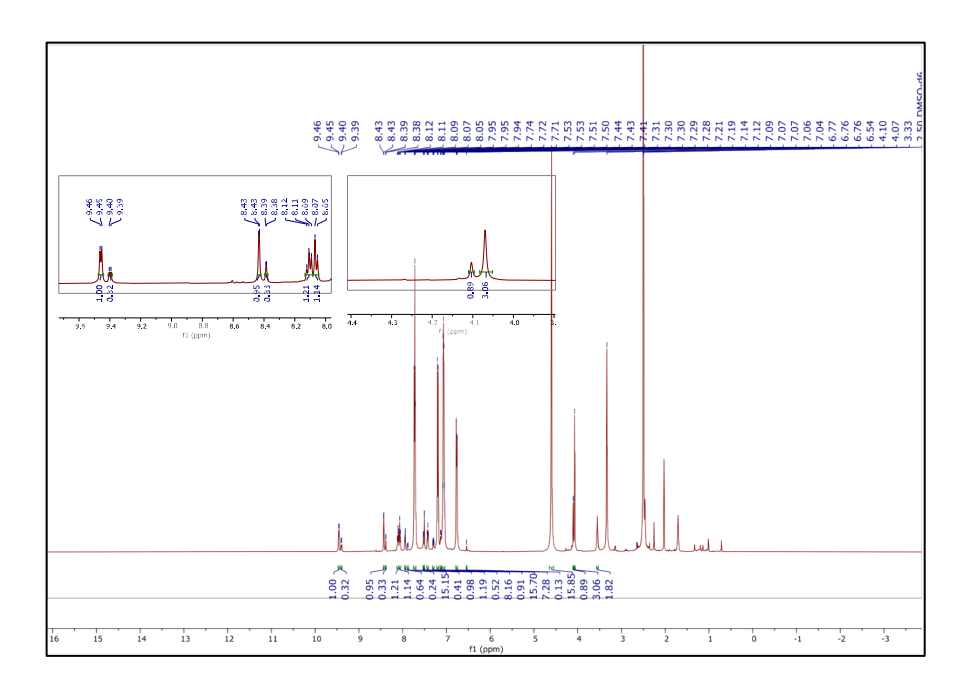


Fig37. ¹H NMR spectra of Ru8 and Ru8'

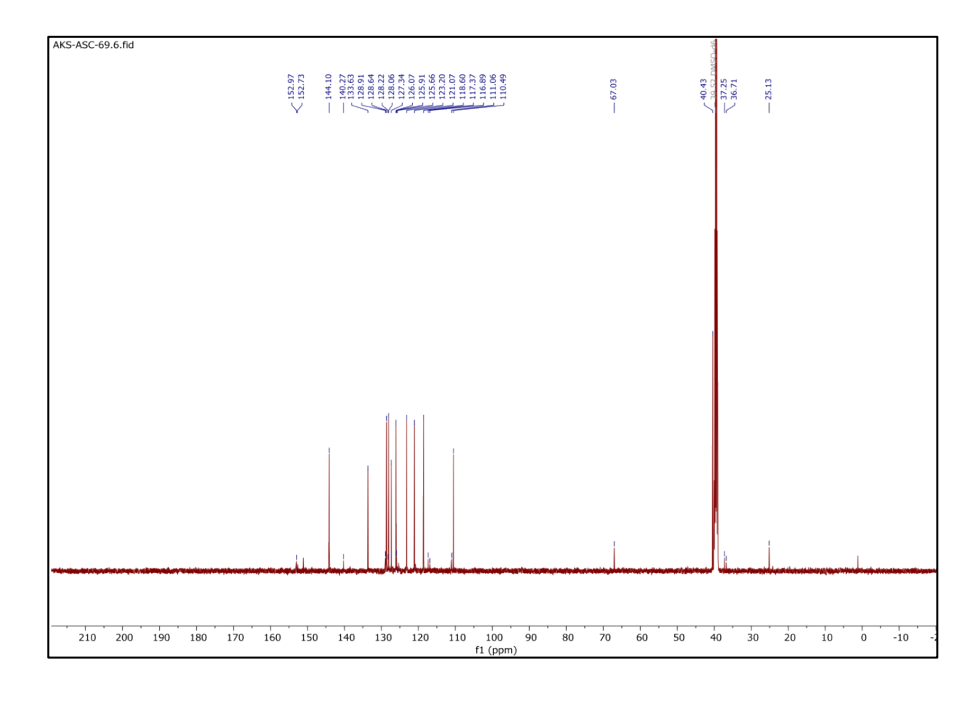


Fig38. ¹³C{¹H} NMR spectra of Ru8 and Ru8'

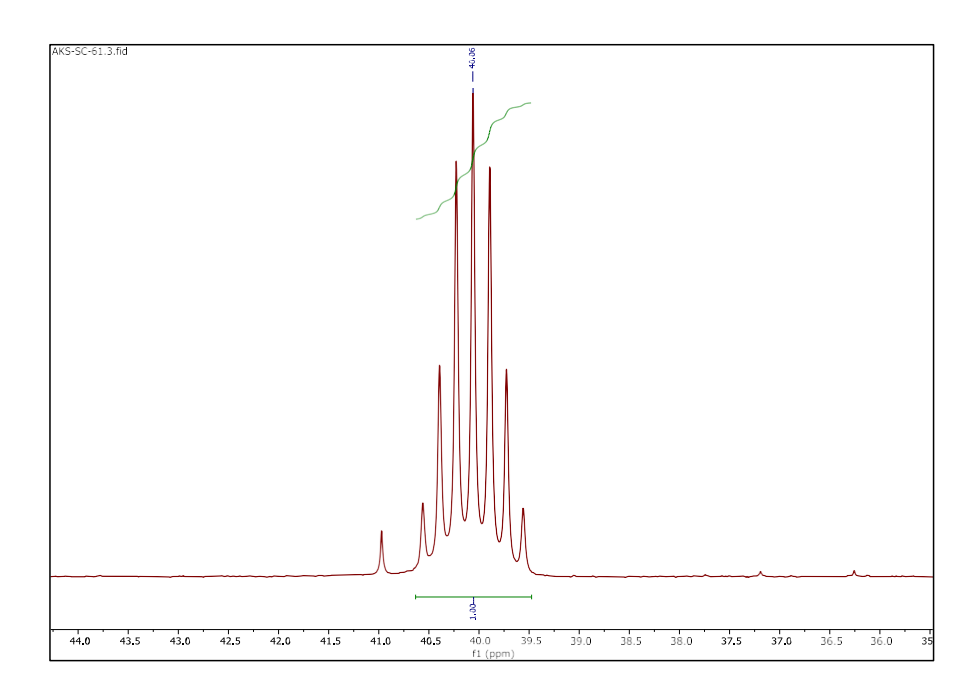


Fig39. ³¹P{¹H} NMR spectra of Ru8 and Ru8′

CHAPTER-4

4.1 **CONCLUSION:**

In summary, the diastereomeric complexes Ru8 and Ru8' were successfully synthesized and characterized in the laboratory through various spectroscopic techniques. The characterization was conducted using multiple analytical methods including ¹H, ¹³C, and ³¹P NMR spectroscopy, whereby the existence of a 3:1 diastereomeric ratio was observed in the ¹H NMR spectra. Initially, concerns were raised regarding the aliphatic region peaks; however, it was determined that these signals were attributed to S-BINAM decomposition, which was also detected in the NMR spectra through its characteristic peaks. The synthesis represents a significant advancement following numerous unsuccessful attempts with various precursors and chiral auxiliaries. Moving forward, reaction conditions must be optimized to improve yield and diastereoselectivity. Additionally, potential applications across various fields need to be investigated to fully utilize these novel ruthenium complexes. The catalytic, photochemical, and biological properties of these diastereomeric pairs should be evaluated to determine their efficacy in asymmetric synthesis, photocatalysis, or as potential therapeutic agents. Further studies may be directed toward the separation of these diastereomers to assess their individual properties and applications.

4.2 FUTURE PERSPECTIVE:

The successful synthesis and characterization of the diastereomeric ruthenium complexes Ru8 and Ru8' open up a wide array of promising avenues for future research. Moving forward, a primary focus should be placed on optimizing the reaction conditions to enhance both the overall yield and the diastereoselectivity, which could lead to more efficient production and a better understanding of the factors influencing selectivity. Additionally, the separation and isolation of individual diastereomers will be crucial for in-depth studies of their unique chemical and physical properties. Exploring the catalytic activity of these complexes in asymmetric synthesis could reveal valuable applications in the preparation of enantioenriched compounds, which are of great interest in pharmaceutical and fine chemical industries. Furthermore, investigating their photochemical properties may uncover novel uses in photocatalysis or light-driven transformations, while their potential as therapeutic agents warrants comprehensive biological evaluation. Such studies could include cytotoxicity assays, mechanismof-action analyses, and structure- activity relationship investigations. Overall, the groundwork laid by the initial synthesis and characterization of Ru8 and Ru8' provides a strong platform for multidisciplinary research, with the potential to impact catalysis, materials science, and medicinal chemistry.

REFERENCES

- (1) Kazushi Mashima; Kusano, K.; Ohta, T.; Ryoji Noyori; Hidemasa Takaya. Synthesis of New Cationic BINAP–Ruthenium(II) Complexes and Their Use in Asymmetric Hydrogenation [BINAP = 2,2'-Bis(Diphenylphosphino)-1,1'-Binaphthyl]. *Journal of the Chemical Society Chemical Communications* **1989**, No. 17, 1208–1210.
- (2) Szabó, Z.; Attila Paczal; Tibor Kovács; Attila Mándi; Andras Kotschy; Tibor Kurtán. Synthesis and Vibrational Circular Dichroism Analysis of N-Heterocyclic Carbene Precursors Containing Remote Chirality Centers. *International Journal of Molecular Sciences* **2022**, *23* (7), 3471–3471.
- (3) Li, W.; Wagener, T.; Hellmann, L.; Daniliuc, C. G.; Mück-Lichtenfeld, C.; Neugebauer, J.; Glorius, F. Design of Ru(II)-NHC-Diamine Precatalysts Directed by Ligand Cooperation: Applications and Mechanistic Investigations for Asymmetric Hydrogenation. *Journal of the American Chemical Society* 2020, 142 (15), 7100–7107.
- (4) Mezzetti, A. Ruthenium Complexes with Chiral Tetradentate PNNP Ligands: Asymmetric Catalysis from the Viewpoint of Inorganic Chemistry. **2010**, *39* (34), 7851–7851.
- (5) Carmona, D.; Elipe, S.; Lahoz, F. J.; Oro, L. A.; Cativiela, C.; López-Ram, P.; M. Pilar Lamata; Vega, C.; Viguri, F. Chiral Ruthenium Complexes as Catalysts in Enantioselective Diels-Alder Reactions. Crystal Structure of the Lewis Acid-Dienophile Adduct. *Chemical Communications* 1997, No. 24, 2351–2352.
- (6) Sahli, Z.; Derrien, N.; Pascal, S.; Demerseman, B.; Roisnel, T.; Barrière, F.; Achard, M.; Bruneau, C. Preparation of Chiral Ruthenium(Iv) Complexes and Applications in Regio- and Enantioselective Allylation of Phenols. *Dalton Transactions* 2011, 40 (20), 5625.
- (7) Bootsma, J.; Guo, B.; Johannes; Otten, E. Ruthenium Complexes with PNN Pincer Ligands *Dalton Transactions* **2012**, *40* (20), 5625.

- (8) Consiglio, Giambattista.; Morandini, Franco. Half-Sandwich Chiral RutheniumComplexes. *Chemical Reviews* **1987**, *87* (4), 761–778.
- (9) Balou, S.; Athanasios Zarkadoulas; Koukouvitaki, M.; Marchiò, L.; Efthimiadou, E. K.; Mitsopoulou, C. A. Synthesis, DNA-Binding, Anticancer Evaluation, and Molecular Docking Studies of Bishomoleptic and Trisheteroleptic Ru-Diimine Complexes Bearing 2-(2-Pyridyl)-Quinoxaline. *Bioinorganic Chemistry and Applications* 2021, 2021, 1–16.
- (10) Noyori, A.; Hashiguchi, S. Asymmetric Transfer Hydrogenation Catalyzed by Chiral Ruthenium Complexes. *Accounts of Chemical Research* **1997**, *30* (2), 97–102.
- (11) James, B. R.; Daniel; Voigt, R. F. Catalytic Asymmetric Hydrogenation Using Ruthenium(II) Chiral Phosphine Complexes. *Journal of the Chemical Society Chemical Communications* **1975**, No. 14, 574–574.
- (12) Ikariya, T.; Ishii, Y.; Kawano, H.; Arai, T.; Saburi, M.; Yoshikawa, S.; Akutagawa, S. Synthesis of Novel Chiral Ruthenium Complexes of 2,2'-Bis(Diphenylphosphino)-1,1'-Binaphthyl and Their Use as Asymmetric Catalysts. *J. Chem. Soc., Chem. Commun.* **1985**, No. 13, 922–924.
- (13) Vogel, P.; Houk, K. N. *Organic Chemistry: Theory, Reactivity and Mechanisms in Modern Synthesis*; John Wiley & Sons, 2019.
- (14) Glorius, F. *N-Heterocyclic Carbenes in Transition Metal Catalysis*; Springer, 2007.
- (15) Cornils, B.; Herrmann, W. A.; Beller, M.; Paciello, R. Applied Homogeneous Catalysis with Organometallic Compounds: A Comprehensive Handbook in Four Volumes; John Wiley & Sons, 2017.
- (16) Hopkinson, M. N.; Richter, C.; Schedler, M.; Glorius, F. An Overview of N-Heterocyclic Carbenes. *Nature* **2014**, *510* (7506).
- (17) Sadig Aghazada; Zimmermann, I.; Valeriu Scutelnic; Nazeeruddin, M. K. Synthesis and Photophysical Characterization

- of Cyclometalated Ruthenium Complexes with N-Heterocyclic Carbene Ligands. *Organometallics* **2017**, *36* (13), 2397–2403.
- (18) de Frémont, P.; Marion, N.; Nolan, S. P. Carbenes: Synthesis, Properties, and Organometallic Chemistry. *Coordination Chemistry Reviews* **2009**, *253* (7-8), 862–892.
- (19) Soleilhavoup, M.; Bertrand, G. Cyclic (Alkyl)(Amino)Carbenes (CAACs): Stable Carbenes on the Rise. *Acc. Chem. Res.* **2015**, *48* (2), 256–266.
- (20) Grisi, F.; Costabile, C.; Gallo, E.; Mariconda, A.; Tedesco, C.; Longo, P. Ruthenium-Based Complexes Bearing Saturated Chiral N-Heterocyclic Carbene Ligands: Dynamic Behavior and Catalysis. *Organometallics* 2008, 27 (18), 4649–4656.
- (21) Ye, C.-X.; Meggers, E. Chiral-At-Ruthenium Catalysts for Nitrene-Mediated Asymmetric C–H Functionalizations. *Accounts of Chemical Research* **2023**, *56* (9), 1128–1141.
- (22) Catalano, A.; Mariconda, A.; Sinicropi, M. S.; Ceramella, J.; Iacopetta, D.; Saturnino, C.; Longo, P. Biological Activities of Ruthenium NHC Complexes: An Update. *Antibiotics* 2023, 12 (2), 365.
- (23)Zhang, Z.; Mei, W.; Wu, X.; Wang, X.; Wang, B.; Chen, S. Synthesis and Characterization of Chiral Ruthenium(II) Complexes Λ/Δ-[Ru(Bpy)₂(H₂Iip)](ClO₄)₂ as Stabilizers of *C-Myc* G-Quadruplex DNA. *Journal of Coordination Chemistry* **2015**, 68 (8), 1465–1475.
- (24) Glorius, F.; Gnas, Y. Chiral Auxiliaries Principles and Recent Applications. *Synthesis* **2006**, *2006* (12), 1899–1930.
- (25) Heravi, M. M.; Zadsirjan, V.; Farajpour, B. Applications of Oxazolidinones as Chiral Auxiliaries in the Asymmetric Alkylation Reaction Applied to Total Synthesis. *RSC Advances* **2016**, *6* (36), 30498–30551.

- (26) Diaz-Muñoz, G.; Miranda, I. L.; Sartori, S. K.; Rezende, D. C.; Alves Nogueira Diaz, M. Use of Chiral Auxiliaries in the Asymmetric Synthesis of Biologically Active Compounds: A Review. *Chirality* **2019**, *31* (10), 776–812.
- (27) Barton, J. K.; Basile, L. A.; Danishefsky, A.; Andrei Alexandrescu. Chiral Probes for the Handedness of DNA Helices: Enantiomers of Tris(4,7-Diphenylphenanthroline)Ruthenium(II). *Proceedings of the National Academy of Sciences of the United States of America* 1984, 81 (7), 1961–1965.
- (28) Haq, I.; Lincoln, P.; Suh, D.; Bengt Nordén; Chowdhry, B. Z.; Chaires, J. B. Interaction of .DELTA.- and .LAMBDA.-[Ru(Phen)2DPPZ]2+ with DNA: A Calorimetric and Equilibrium Binding Study. *Journal of the American Chemical Society* **1995**, *117* (17), 4788–4796.
- (29) Herrero, S.; Usón, M. A. A Straightforward Method for Assigning Stereochemical Λ/Δ Descriptors to Octahedral Coordination Compounds. *Journal of Chemical Education* **1995**, 72 (12), 1065–1065.
- (30) Svensson, F. R.; Abrahamsson, M.; Niklas Strömberg; Ewing, A. G.; Lincoln, P. Ruthenium(II) Complex Enantiomers as Cellular Probes for Diastereomeric Interactions in Confocal and Fluorescence Lifetime Imaging Microscopy. *The Journal of Physical Chemistry Letters* **2011**, *2* (5), 397–401.
- (31) Flamme, M.; Clarke, E.; Gasser, G.; Hollenstein, M. Applications of Ruthenium Complexes Covalently Linked to Nucleic Acid Derivatives. *Molecules* **2018**, *23* (7), 1515–1515.
- (32) Cardin, C. J.; Kelly, J. M.; Quinn, S. J. Photochemically Active DNA-Intercalating Ruthenium and Related Complexes – Insights by

- Combining Crystallography and Transient Spectroscopy. **2017**, *8* (7), 4705–4723.
- (33) Ashby, M. T.; Govindan, G. N.; Grafton, A. K. Kinetics and Mechanism of the Facile Diastereomeric Isomerization of a Tris(Bidentate)Ruthenium(II) Complex Bearing a Misdirected Bipyridyl Ligand: DELTA...LAMBDA.-(.Delta./.Lambda.-1,1'-Biisoquinoline)Bis(2,2'-Bipyridine)Ruthenium(II). *Inorganic Chemistry* **1993**, *32* (18), 3803–3804.
- (34) Claessens, N.; Pierard, F.; Bresson, C.; Moucheron, C.; Kirsch-De Mesmaeker, A. Optically Active Ru(II) Complexes with a Chiral Tröger's Base Ligand and Their Interactions with DNA. *Journal of Inorganic Biochemistry* **2007**, *101* (7), 987–996.
- (35) Fletcher, N. C.; Keene, F. R.; Viebrock, H.; Zelewsky, A. von. Molecular Architecture of Polynuclear Ruthenium Bipyridyl Complexes with Controlled Metal Helicity. *Inorganic Chemistry* **1997**, *36* (6), 1113–1121.
- (36) Flamme, M.; Clarke, E.; Gasser, G.; Hollenstein, M. Applications of Ruthenium Complexes Covalently Linked to Nucleic Acid Derivatives. *Molecules* **2018**, *23* (7), 1515–1515.
- (37) Myari, A.; Hadjiliadis, N.; Garoufis, A. Synthesis and Characterization of the Diastereomers Λ- and Δ-[Ru(Bpy)2(M-Bpy-l-Arg-Gly-l-Asn-l-Ala-l-His-l-Glu-l-Arg)]Cl2. *Journal of Inorganic Biochemistry* **2005**, *99* (2), 616–626.
- (38) Browne, W. R.; O'Connor, C. M.; Villani, C.; Vos, J. G. Separation and Photophysical Properties of the ΔΔ, ΛΛ, ΔΛ, and ΛΔ Stereoisomers of a Dinuclear Ruthenium(II) Complex. *Inorganic chemistry* **2001**, *40* (21), 5461–5464.
- (39) Saha, A.; Nath, S.; Yadav, E.; Singh, A. K. Ru(II)-Protic-NHC Complex Catalyzed Selective N-Alkylation of Anilines with Primary Alcohols: Mechanistic Insights and Role of Salt Additives. *ChemCatChem* **2025**, *18*,1867-3880.

- (40) Mühlen, C.; Linde, J.; Rakers, L.; Tan, T. T. Y.; Kampert, F.; Glorius, F.; Hahn, F. E. Synthesis of Iron(0) Complexes Bearing Protic NHC Ligands: Activity. *Organometallics* **2019**, *38* (12), 2417–2421.
- (41) Steffen Cepa; Schulte, C.; Florian Roelfes; Hahn, F. E. Hydrogen Activation by an Iridium(III) Complex Bearing a Bidentate Protic NH,NR-NHC^Phosphine Ligand. *Organometallics* **2015**, *34* (22), 5454–5460.
- (42) Ryoji Noyori. Chiral Metal Complexes as Discriminating Molecular Catalysts. *Science* **1990**, *248* (4960), 1194–1199.
- (43) Kaoru Fuji; Manabu Node; Tanaka, F.; Shinzo Hosoi. Binaphthol as a Chiral Auxiliary. Asymmetrical Alkylation of Arylacetic Acid. *Tetrahedron Letters* **1989**, *30* (21), 2825–2828.
- (44) Miyashita, A.; Yasuda, A.; Hidemasa Takaya; Koshiro Toriumi; Ito, T.; T. SOUCHI; Ryoji Noyori. Synthesis of 2,2'-Bis(Diphenylphosphino)-1,1'-Binaphthyl (BINAP), an Atropisomeric Chiral Bis(Triaryl)Phosphine, and Its Use in the Rhodium(I)-Catalyzed Asymmetric Hydrogenation of .Alpha.-(Acylamino)Acrylic Acids. 1980, 102 (27), 7932–7934.
- (45) Srivastava, N.; Meena, R.; Singh, A. K. Phosphine-Free Ru(II)-CNC Pincer Complexes with Mixed Protic- and Classical-NHCs in the Same Molecule for Hydrogen Production via Oxidant-Free Benzyl Alcohol Dehydrogenation to Benzoic Acids. *New Journal of Chemistry* **2024**, *53*, 12662-12675.
- (46) Shahid, N.; Singh, A. K. Unravelling the Kinetics of Electro- and Photochemical S→O Linkage Isomerization in Ru(II)-NHC-DMSO Complexes Utilised for Photoinduced Substitution Reactions. *Dalton Transactions* **2024**. *53*, 6870-6874.